Basal Area Growth and Crown Dynamics in a Loblolly Pine Spacing Trial

Philip J. Radtke

Thesis submitted to the faculty of the
Virginia Polytechnic Institute and State University
in partial fulfillment of the requirements for the degree of
Master of Science
in
Forestry

APPROVED:

_____
Harold E. Burkhart, Chair

_____ _____
Timothy G. Gregoire Shepard M. Zedaker

August 2, 1996
Blacksburg, Virginia

Basal Area Growth and Crown Dynamics in a Loblolly Pine Spacing Trial

Philip J. Radtke

(ABSTRACT)

Relationships between the culmination of basal area growth and degree of crown closure in loblolly pine (*Pinus taeda* L.) were investigated. A spacing trial established on the lower Appalachian Piedmont and Atlantic Coastal Plain provided the data for the investigation. Test plots were planted at densities ranging from 303 to 2723 stems per acre, and at various rectangular and square spacings. Annual stem and crown measurements were used to derive the sought-after relationships.

The age of basal area culmination was found to be inversely related to both planting density and site index. Crown closure was advanced on sites of relatively high quality, exhibiting an approximately linear increase with time from planting until the age of basal area culmination. The slope of this trend increased with planting density. The degree of crown closure at the age of basal area culmination was significantly higher on narrowly-spaced plots than it was on widely-spaced plots; however, it did not vary significantly with site index. Although crown closure is generally accelerated on high quality sites, the relatively early culmination of basal area growth on such sites offsets the increase - the net result being that crown closure at culmination age does not vary significantly with site differences.

Crown closure indices can be used to determine whether or not a stand has reached the culmination of basal area growth; however, more readily available information on spacing and site index can be used to make the same prediction. The results of this study might be most useful to modelers of early stand dynamics in loblolly pine and other commercially important pines.

ACKNOWLEDGMENTS

I offer my sincere thanks to Dr. Harold Burkhart for giving me the opportunity to pursue this thesis. I always appreciated your insight, direction, patience, and conversation. Thanks also to Drs. Timothy Gregoire and Shep Zedaker, who served on my thesis committee. Working with you has helped make my stay at VPI an extremely rewarding experience for me. I look forward to continued friendship and association with you for years to come. I gratefully acknowledge Ralph Amateis for offering me advice regarding various projects I've worked on at VPI, and for helping me to obtain and interpret the data used in this study. My thanks to the members of the Loblolly Pine Growth and Yield Research Cooperative who supported me financially throughout my degree program.

I wish to thank Ms. Mildred Flythe and the rest of my family for supporting and enduring my drive to reach this goal. Finally, to my closest friends: Oliver, Lisa, Hunter, Mike, Scooter, and Tracy; your companionship was the highlight of these past two years - time that went by much too fast because I spent it with all of you.

TABLE OF CONTENTS

LIST OF FIGURES

LIST OF TABLES

Chapter 1

INTRODUCTION

Competition is one of the most dynamic forces that shape forest stands. Its influence on growth and yield is an important consideration to forest managers, as the processes of growth and competition are virtually inseparable in the application of forestry. Scientists have continually made efforts at developing and refining models of competition. The ultimate goal of these efforts can be seen as the enhancement of competition-yield theory, which will serve as a basis for sound management decisions. The research proposed here will focus extensively on the culmination age of basal area growth in a forested monoculture and examine how culmination age is related to intraspecific competition as indicated by several crown closure indices.

A primary rationale for studying the age of basal area growth culmination is that it typically occurs outside the range of prediction of volume-yield models. Basal area growth seldom, if ever, culminates after the time when pulpwood merchantability limits are first reached. Yet, growth and yield models, by necessity, must represent basal area growth in the pre-merchantable stages of stand development. Even though a great deal is understood about the growth of young stands, it is often difficult to predict such growth - partly because of the high variability in the growth of young trees, and partly because of a lack of adequate predictor variables. The result is that modelers sometimes fail to incorporate what is known about the early stages of basal area growth into their models.

The high quality of data available to this study made it possible to confront the problems of high variability and a lack of predictor variables. Particular attention was paid to establishing a uniform growing environment for loblolly pine (*Pinus taeda* L.) on the spacing trials which supply the data for this research. The resulting stands are remarkably consistent in their growth and responses to the various spacing treatments, even at very young ages.

Extensive crown and stem measurements were made on an annual basis for the first twelve years after planting - corresponding directly with the range over which basal area growth normally culminates in loblolly pine. The availability of crown measurements was a tremendous asset to the study in that it preserved a record of competition for growing space among neighboring trees. The spacing trial data provided an excellent source of information from which to examine the effects of such competition on basal area growth of young trees, and the extent to which it can be predicted by crown closure indices.

OBJECTIVES

The main objective of this work was to investigate relationships between several measures of crown closure and the basal area growth of young loblolly pine. The following is a list of specific objectives developed prior to the start of the investigation:

1. Develop a set of basal area curves to estimate the age of basal area growth culmination in loblolly pine.

2. Determine the influence of spacing on the age of basal area growth culmination, and the age when basal area growth is slowed by competition.

3. Derive crown area projection, crown closure, and crown overlap indices from ground-level crown measurements. Include a brief analysis of the effect of edge bias on these derivations.

4. Determine how well crown closure indices predict the age of culmination of basal area growth or the onset of competition.

Chapter 2
LITERATURE REVIEW

Modeling Basal Area Growth

Basal area growth, like many other plant growth relationships, is often expressed in one of two ways, as cumulative growth, or as incremental (i.e. instantaneous) growth. Cumulative basal area growth is generally sigmoidal, that is, S-shaped, when plotted graphically versus age. Such graphs are commonly called growth curves. Alternatively, instantaneous growth curves show the current rate of basal area growth at any point in time. To distinguish them from cumulative growth curves, these are often referred to as increment, current annual growth, or growth rate curves (Husch et al. 1982, Seber and Wild 1989, Avery and Burkhart 1994).

Growth Curves

Modelers have focused a great deal of attention on the development of mathematical representations of growth, and many of these functions describe diameter growth well (Zeide 1989). A number of authors have examined their various behaviors and interpretations of their parameters, and fitting procedures (Hunt 1982, Bates and Watts 1988, Seber and Wild 1989, Sit and Poulin-Costello 1994).

These models have various properties besides their characteristic sigmoid curve. They take some initial value - generally zero - at an initial age, increase at an increasing rate until some inflection point, then increase at a decreasing rate as they approach a horizontal asymptote. Depending upon the number and arrangement of parameters in the model, the curves are flexible in terms of their initial value, rate of increase, shape, and upper limit.

A growth model used widely in forestry applications is the Richards generalization of Von Bertalanffy's (1938) model. The Richards model is also denoted the Chapman-Richards model, because D. G. Chapman and F. J. Richards concurrently published their views that Von Bertalanffy's model was too specific. Chapman (1961) made this remark based on his experience with allometric relationships of fish. Richards (1959) demonstrated the need for the generalization using data from the botanical literature.

Von Bertalanffy formulated his model by following Pütter's (1920) reasoning that the growth of an organism is "given by the difference between the processes of building up and breaking down" (Von Bertalanffy 1957). His expression for this process was

$$dW/dt = \eta W^m - \kappa W^n \qquad (1)$$

where

dW/dt - change in organism weight (W) over time (t)
η - constant of anabolism

κ - constant of catabolism
m, n - allometric constants

A primary assumption of Von Bertalanffy (1938, 1957) is that the catabolic rate is directly proportional to an organism's weight. The allometric constant of catabolism, n, is unity under this assumption. Von Bertalanffy (1957) identified three distinct growth types: anabolic growth rate proportional to the organism's surface area (m = 2/3); anabolic growth rate directly proportional to weight (m=1); and anabolic growth rate proportional to an intermediate value ($2/3 < m < 1$).

Richards (1959) showed that relaxing Von Bertalanffy's restrictions on m gave a more general model which, although perhaps theoretically problematic, is empirically flexible. He showed that the function is equivalent to the monomolecular, autocatalytic (logistic), exponential, and Gompertz models for specific integer values of m. Furthermore, he argued, m should be flexible to take intermediate real values or values greater than one, in order to accurately represent real data. The Richards model is often expressed in the form

$$W = a\left[1 - e^{b(Age - A_o)}\right]^c \qquad (2)$$

where a, b, and c are expressions of Von Bertalanffy's growth rate parameters.

$a = \left(\frac{\eta}{\kappa}\right)^{\frac{1}{1-m}}$
$b = -\kappa(1 - m)$
$c = \frac{1}{1 - m}$

and

Age - organism age
A_o - age at which organism takes some initial value W_o (here $W_o = 0$)
e - the base of the natural logarithm

The Richards model has been used extensively in American forestry because it has proven to be relatively accurate and empirically flexible (Zeide 1989, 1993). In addition to an organism's weight (W), Richards noted that the model equally applies to state variables that have fixed allometric relationships with W. Pienaar and Turnbull (1973) demonstrated the fixed allometric relationships between dbh, height, and volume of spruce trees. They reported that the Richards model also worked well when fit to basal area, height, and volume data.

Schnute (1981) introduced a further generalization of the family of growth models including the Richards, logistic, and Gompertz functions. Schnute's model is based on the acceleration of growth - the second derivative of size with respect to age - compared to earlier differential models based simply on the growth rate. Schnute's model describes the size of an organism as a function of its age, including its estimated size (Y) at the beginning and end of the interval over which the model is applied.

$$Y = \left[y_1^{\frac{1}{c}} + \left(y_2^{\frac{1}{c}} - y_1^{\frac{1}{c}} \right) \frac{1 - e^{b\,(Age - T_1)}}{1 - e^{b\,(T_2 - T_1)}} \right]^c \qquad (3)$$

where

b,c - growth rate parameters $\equiv$ Eq. (2)

T_1 - beginning of the modeling interval, typically, the time of initial measurement

T_2 - end of the modeling interval, typically, the time of final measurement

y_1,y_2 - estimated sizes at times T_1 and T_2

Bredenkamp and Gregoire (1988) showed that Schnute's model could be used to describe dbh growth of *Eucalyptus grandis* where growth did not follow the typical sigmoidal behavior. Huang et al. (1992) used the Schnute model to describe height-diameter relationships, and proposed that the model would be useful if extended into other forestry applications, such as the study of basal area-age relationships.

The Schnute model is flexible to fit non-sigmoidal growth, but for a particular range of the shape parameters ($b < 0$ and $c > 1$), the model is algebraically equivalent to the Richards model (Schnute 1981). For other values of b and c, however, the function may indicate growth free of an upper asymptote, inflection point, intersection with the x-axis at an initial age, or any combinations thereof.

Increment Curves

Basal area increment curves show the rate of growth as a function of age. Mathematically, an increment function is the derivative of its growth curve with respect to age. Conversely, the integral of a basal area increment curve with respect to age is the basal area growth curve. For sigmoidal growth, increment curves are unimodal, take an initial value of zero at age A_o, rise to a maximum value at the age of the growth curve's inflection point, then decrease asymptotically toward zero.

Several model forms are available that represent basal area increment efficiently, however, they do not necessarily possess closed-form solutions of the integral with respect to age. Where necessity dictates working with both the cumulative and incremental forms of a basal area curve, it may be most efficient to select a growth function in its cumulative form, and obtain the increment function as the derivative with respect to age. Derivatives of many growth curves are given in modeling texts (e.g. Hunt 1982, Sit and Poulin-Costello 1994) or may be computed directly using elementary calculus. Differentiating the Richards and Schnute models with respect to age, for example, give Eqs. (4a), and (b), respectively.

$$\frac{\partial BA}{\partial Age} = -abc \bullet e^{b(Age - A_o)} \left[1 - e^{b(Age - A_o)} \right]^{[c-1]} \qquad (4a)$$

$$\frac{\partial BA}{\partial Age} = -bc \bullet \frac{\left(y_2^{\frac{1}{c}} - y_1^{\frac{1}{c}}\right) e^{b(Age - T_1)}}{1 - e^{b(T_2 - T_1)}} \left[y_1^{\frac{1}{c}} + \left(y_2^{\frac{1}{c}} - y_1^{\frac{1}{c}}\right) \frac{1 - e^{b(Age - T_1)}}{1 - e^{b(T_2 - T_1)}} \right]^{c-1} \quad (4b)$$

As previously noted, cumulative and incremental growth curves are interchangeable by the processes of differentiation and integration. This property does not, however, imply that cumulative growth and increment curves may be fitted to data interchangeably with identical results. Differences in fitting growth and increment equations to data might be caused by growth rates that vary during the time interval over which observations were taken. As Hunt (1982) points out, only truly instantaneous measurements may be represented as single points along an increment curve. In the case of basal area increment observations derived from periodic stem remeasurements, the observations are not truly instantaneous, but only average growth rates estimated over the length of the remeasurement period.

For a measurement interval of one year, variations in growth rate occur due to seasonal changes. Assmann (1970) describes the annual progress of radial stem growth of temperate-climate tree species, noting that stem size is essentially constant during dormancy, but increases sigmoidally during the growing season to an upper constant where it remains fixed until the following growing season. Kramer (1943) presented evidence that loblolly pine height growth is nearly linear from April to August, with a small amount of additional height growth in late fall, and no height growth during the rest of the year.

Within a growing season, height growth of pines occurs in distinguishable stages known as flushes (Lanner 1976). Boyer (1970) documented cyclical patterns of flush elongation. His results showed that while the newest flush of terminal buds is beginning its elongation cycle, the previous flush is near the completion of its cycle. These periods of flush elongation overlap. This idea was verified by Griffing and Elam (1971) who showed that the overlapping growth of consecutive flushes results in a nearly constant growth rate along the total shoot axis during the midseason months.

Seasonal and periodic growth cycles are ignored by growth curves that effectively smooth out seasonal variations and treat growth as a continually occurring phenomenon. Pienaar and Turnbull (1973) argue that such simplifications need not nullify the adequacy of growth models. Rather, their merit should be judged on the ability to represent general patterns in relation to specific purposes.

Culmination of Basal Area Growth

The point at which an increment curve reaches its maximum value is equivalent to the inflection point of a growth curve, and is known as the culmination of basal area increment. Previous studies of the inflection point of basal area growth curves have attempted to determine its relationship to stocking density, and the onset of competition effects in forest stands.

Assmann (1970) noted that the basal area increment is closely related to individual trees' available growing space, in that basal area increment typically increases in young trees until their maximum useable growing space is reached. Furthermore, Assmann observed larger basal area increments in trees with large growing spaces than in trees grown on smaller spaces. These ideas were investigated by Pienaar and Turnbull (1973), who found that the age of culmination of basal area increment was inversely related to initial stocking density.

In developing their basal area growth model, Harrison and Daniels (1987) suggested that the inflection point of the curve indicates inter-tree crown competition and the start of density-dependent mortality. They used this idea to distinguish between pre- and post-competitive life stages in loblolly pine stands in order to apply separate mortality models.

The age of a growth curve's inflection is found by taking the second partial derivative of the function with respect to age. When this second derivative is set to zero, solving for age gives A*, the age at which the curve's inflection point occurs. The age of inflection for the Richards model is given in Eq. (5).

$$A^* = A_o + \frac{1}{b}\ln\left(\frac{1}{c}\right) \qquad (5)$$

Assmann (1970) noted that basal area increment culminates early in the life of a stand relative to the age at which merchantable volume first develops. In the development of yield tables, then, culmination of the basal area increment was a fairly unimportant consideration. More sophisticated approaches could explicitly formulate models in terms of basal area culmination, use culmination age information as a guide for choosing an initial spacing, or for some other purpose, such as determination of the onset of intraspecific competition.

Modeling Canopy Closure

The term "crown closure" has been used in the literature to convey two meanings related to the dynamics of between-tree crown competition. Spurr (1960) defined crown closure as "the proportion of the area of a stand or other homogeneous unit covered by the crowns of the trees." By this definition, crown closure is simply a number ranging between [0, 1], and could be considered an "index" of crown closure. The second meaning of crown closure can be inferred from the context of authors (e.g. Strub et al. 1975, Harrison and Daniels 1987) who use the term to signify the event whereby neighboring tree crowns begin to either touch, overlap, or exert competition pressure on each other. The former meaning of crown closure will be used throughout this paper unless otherwise noted.

Crown closure is measured either from ground-level or from overhead. In general, ocular or photographic methods (Lemmon 1956, Evans and Coombe 1959, Daubenmire 1959, James and Shugart 1970) are used to make ground-level crown closure observations, while aerial photography is used to make the measurements from overhead. Crown measurements made from aerial photography may give somewhat different results than ground-level measurements

depending on a host of conditions: shading; photo scale and resolution; stand density; and whether measurements are made of the crowns themselves or the gaps between the crowns (Spurr 1960, Avery and Burkhart 1994). Furthermore, the effort required in obtaining ground-level crown width measurements may be prohibitive (Burton and Shoulders 1982).

Spurr (1960) describes a number of techniques for obtaining crown closure estimates from aerial photography. One approach involves comparing aerial photography from a stand of unknown canopy closure with stereograms from stands of known density in order to make a crown closure classification. Similarly, crown density scales may be used as a basis for comparison. Point sampling may be employed when large scale photography is available. This technique involves laying a transparent dot-grid or similar sampling device over a photograph. Crown closure is then computed as the proportion of dots falling on live tree crowns.

Crown closure may also be derived from aerial photography by summing individual trees' crown areas over a stand. Mitchell (1975) took this approach in digitizing low-level aerial photography of white spruce crowns onto a map grid representing ground units one square foot in area. A component of Mitchell's model relevant to the current study is his method of dealing with trees near the edges of plot boundaries. Since trees outside the study plots were not measured, it was necessary to compensate for areas in the study plots which were actually covered by the live crowns of off-plot trees.

Monserud and Ek (1974) addressed a similar problem they called edge bias, a problem which arises in computing single-tree competition indices for trees near the plot boundary. They discussed several ways of compensating for edge bias - among them, reflection and translation. In reflection a "reflection line" is drawn parallel to the plot boundary running through the center of an edge tree. Trees on the plot are then reflected to positions outside the plot. A variation on the reflection method involves placing the reflection line on the plot boundary rather than through the center of the edge tree. This technique was considered less desirable by Monserud and Ek (1974), based on the result that large boundary trees would be placed adjacent to identically large-sized neighbors; conversely, small boundary trees would have small neighbors.

Translation involves the placement of duplicates of the measured plot around each of its four sides and four corners. The effect of translation is that trees inside the plot boundary at one edge are repeated outside the boundary at the opposite edge. Mitchell (1975) used plot translation to compensate for edge-bias in his crown-mapping study. A number of other single-tree modelers used translation in a similar application, that of calculating single-tree competition indices (Arney 1972, Ek and Monserud 1974, Daniels and Burkhart 1975). These indices involve the mapping of tree influence areas, which are often closely related to crown area projections (Bella 1971). Bella dealt with what he called the "border effect" by eliminating as subjects those trees near the border of the plot.

Another method involves the use of a random variable in distributing trees outside the plot boundary. In particular, Hatch (1971 referenced by Ek and Monserud 1974) computed mean

and standard deviation for individual tree characteristics (competition indices) on his research plots. These statistics were then used to draw from a normal distribution with the characteristic mean and standard deviation. Values drawn from the normal distribution were assigned to trees within the zone of potential edge bias.

Chapter 3
METHODS

Data

A set of spacing trials for loblolly pine maintained by the Loblolly Pine Growth and Yield Research Cooperative provided the data used in this study. The spacing trials utilize a factorial arrangement of four levels of between-tree spacing: 4, 6, 8, and 12 feet. These levels were randomly assigned to plots in two directions, with 49 trees planted in a 7×7 grid on each plot. This arrangement causes plots to vary in shape and size, with the smallest square plot covering 784 ft^2 and the largest 7056 ft^2. In all, 16 plots comprise the full complement of spacing combinations. Adjacent plots are separated by three rows of guard trees to buffer the effects of changes in spacing. The 16 plots and their guard rows are arranged in a compact block which constitutes one replicate. The arrangement of plots is part of a non-systematic experimental design described by Lin and Morse (1975) and Amateis et al. (1987).

Three replicates were established in 1983 at each of four locations in Virginia and North Carolina. Two locations lie in the Atlantic coastal plain, two in the Piedmont of the Appalachian mountain range. One of the coastal plain sites was re-established in 1984 after high incidence of mortality in the first year. Throughout this paper, the sites established near Appomattox and Keysville, Virginia are called the upper and lower Piedmont sites, respectively. The sites near Roanoke Rapids, North Carolina, and West Point, Virginia are called the upper and lower Coastal Plain sites, respectively.

In each of the annual remeasurements, tree condition was recorded along with observations of diameter[†], height to the base of the live crown, total height, crown width within and between rows, and maximum crown width. On the eleventh remeasurement, only tree condition and dbh were observed at all locations. On the twelfth and most recent remeasurement, crown and height measurements were again taken, according to a data collection schedule that calls for continued annual tree condition and dbh observations, with crown and height measurements to be taken biennially.

Culmination of Basal Area Growth

Determining the age at which basal area increment culminates was a primary objective of this study. To reach this objective, a number of methods were employed. The age at which trees reach breast height was derived from annual height measurements. Ground-line diameter measurements were used to obtain breast-height diameter approximations for young trees. Basal area and its average rate of growth were determined from consecutive dbh measurements.

[†] In measurement years one through five, ground line diameter was used, while diameter at breast height (dbh) was measured annually starting with the fifth remeasurement.

Alternative models were fit to basal area and growth rate data, and fitted parameter values were used to estimate the culmination age.

Determining A_o

Basal area does not begin to accumulate until A_o, the first age at which any tree on the plot crosses the breast height plane. At A_o the basal area of the stand is exactly zero. Specific values of A_o were computed using a linear growth assumption for height growth during the year in which trees first reached breast height. For each tree, height was interpolated between the measurement cycles immediately before and after it first reached breast height. Ages at these measurement cycles are denoted A_b and A_a, respectively. The age of initial basal area was computed as

$$A_o = \left[\frac{4.5 - H_b}{H_a - H_b}\right] + A_b \qquad (6)$$

where H_b and H_a are the heights measured at ages A_a and A_b respectively. A small number of trees crossed breast height after age 5. For these 34 trees, A_o was set to one year before the time when their dbh was first recorded.

Modeling Dbh at Young Ages

In studying the culmination of basal area growth, it was necessary to examine data from very young stands. The first dbh measurements on the Loblolly Pine Growth and Yield Research Cooperative's spacing trials, however, were made five years after planting. At younger ages, only ground-line diameter was observed; therefore, it was necessary to derive dbh from ground-line diameter measurements. The mechanism for deriving the dbh information was a series of assumptions about the breast height stem diameter development in these young trees.

The first assumption made use of A_o values derived by the previously described height-growth interpolation method: dbh was assumed to be zero at age A_o. The ground-line diameter at age A_o, denoted GLD_o was not known exactly for most trees. Its value was derived by considering height and ground-line diameter growth rates to be proportional to each other during the one-year period over which breast height was reached. This consideration made it possible to compute GLD_o as

$$GLD_o = \frac{4.5 - H_b}{H_a - H_b}(GLD_a - GLD_b) + GLD_b \qquad (7)$$

where

H_b - Height measured at age A_b
H_a - Height measured at age A_a
GLD_b Ground-line diameter measured at A_b
GLD_a Ground-line diameter measured at A_a

Figure 1 shows a geometric interpretation of how GLD_o is derived from the available height measurements based on the assumption of proportionality between ground-line diameter and height growth. First, A_o is determined by finding the point between height measurements where H_o = 4.5 ft. Then A_o determines the fraction of the year's GLD increment to be attributed to the periods before and after the tree reaches breast height.

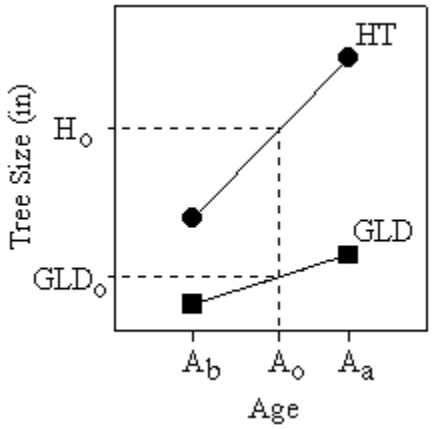

Figure 1. A geometric interpretation of the derivation of ground-line diameter at age A_o. The primary assumption of the method is that height (HT) and GLD grow at rates proportional to each other.

Although the illustration in Fig. 1 shows growth as a constant (linear) process during the year, the method does not impose such a strict condition. Eq. (7) is flexible to allow curvilinear height and GLD growth trends, so long as the trends are proportional to each other. Consider any functions g(A) and h(A) of ground-line diameter and height, respectively. These functions are assumed to be proportional, so, for some constant k, g(A) = kh(A). The inverse of the height growth function h^{-1}(H) can be used to find $A_o = h^{-1}(H_o)$. Then the ground-line diameter at that age is $GLD_o = g(A_o) = g(h^{-1}(H_o)) = g(\frac{1}{k}g^{-1}(H_o)) = \frac{1}{k}(H_o)$. This result is the equivalent of Eq. (7), and is illustrated in Fig. 1 for the special case of the linear functions g(A) and h(A).

A second assumption constrained diameter increments of the derived dbh values to sum to the earliest measured dbh value, DBH_{init}. This constraint is natural in that a tree's diameter at any age is equivalent to the sum of all previous years' diameter increments.

The final assumption related breast height increment to ground line increment for the years between A_o and the age at which the first dbh measurement was taken (A_{init}). By definition, ground line diameter changes from a value of GLD_o at age A_o to a value of GLD_{init} at age A_{init}, and dbh has a measured value of DBH_{init} at age A_{init}. It was assumed that the ratio of breast-height diameter increment (D_{inc}) to ground-line diameter increment (GLDINC) for every year between A_o and A_{init} was a constant for that tree, equal to $\frac{DBH_{init} - DBH_o}{GLD_{init} - GLD_o}$. By a previously

noted assumption, dbh is zero at age A_o ($DBH_o = 0$), so the ratio simplifies to $\frac{DBH_{init}}{GLD_{init} - GLD_o}$. The formula for breast-height diameter increment in any year between A_o and A_{init} is then

$$D_{inc} = GLDINC \times \frac{DBH_{init}}{GLD_{init} - GLD_o} \quad (8)$$

where

D_{inc} - breast-height diameter increment
GLDINC - ground-line diameter increment

Table 1 uses height, ground-line and breast-height diameter measurements from a single tree on the spacing trials to demonstrate the implementation of this formula. From the data in the table and Eq. (7), $GLD_o = \frac{4.5 - 3.0}{5.2 - 3.0}(1.9 - 0.9) + 0.9 = 1.58$. For this tree then, the ratio that will be used to calculate dbh increments for ages between A_o and 5 is $\frac{DBH_{init}}{GLD_{init} - GLD_o} = \frac{2.5}{4.4 - 1.58} = 0.887$. Breast-height diameter increments for ages 3-5 have been tabulated according to this ratio in Table 1 (D_{inc}). Note that the sum of the annual dbh increments does, after rounding, equal the measured dbh at age 5.

The rightmost column in Table 1 shows diameter growth rates adjusted for the time elapsed between dbh measurements. This adjustment is made only for the earliest derived diameter increment value, because in that year stem dbh was accumulated over only a portion of the growing season. The adjustment is computed as the diameter increment divided by the fraction of a year elapsed between A_o and the time at which the ensuing measurement was made.

Table 1. Measured and derived ground-line diameter (GLD), breast-height diameter (DBH), diameter increment (D_{inc}), and dbh growth rate (D_{rate}) for a single tree in the spacing trial data at specified ages. Derived values are printed in boldface type.

Age	Height (ft)	GLD (in)	DBH (in)	D_{inc} (in)	D_{rate} (in)
1	0.9	0.3			
2	3.0	0.9			
A_o= **2.68**	**4.5**	**1.58**	**0.0**	**0.0**	**0.0**
3	5.2	1.9	**0.28**	**0.28**	**0.88**
4	7.7	3.1	**1.34**	**1.06**	**1.06**
5	10.9	4.4	2.5	**1.15**	**1.15**

Deriving Basal Area Information

The derivation of basal area information for curve fitting was a relatively straightforward process, complicated somewhat by the need for estimates of increment rates. Basal area was computed for each tree, by definition, as the cross-sectional area of the stem at breast height, converted to the English units of square feet. The equation for this transformation is $BA = (0.005454154)D^2$, where basal area (BA) is given in square feet, and breast-height diameter (D) measured in inches.

Basal area increment (BA_{inc}) was derived by simply taking the difference between successive basal area observations. For most observations, $BA_{inc} \equiv BA_{rate}$, the average rate of growth of basal area over the measurement interval. This equivalency is due to the fact that the measurements were taken exactly one year apart. In the year during which any tree first reaches breast height, however, BA_{inc} was divided by the proportion of the year during which the tree was taller than 4.5 feet to obtain $BA_{rate} = BA_{inc} \div (A_a - A_o)$. This step is analogous to the calculation of D_{rate} in the previous section.

Computed values of BA_{rate} essentially give the average rate of basal area growth during the measurement interval. By the intermediate value theorem of Calculus, this quantity is exactly equivalent to the basal area growth rate at some time during the interval; however, the exact time at which the two are equivalent is not known in this application. Numerous modelers have considered the midpoint of the interval as a useful approximation. Clutter (1963), for example, considered that actual deviations from the linear growth assumption over a five year interval for loblolly pine would be "inconsequential." Applying such reasoning here, but to a much shorter interval, the age corresponding to any BA_{rate} was computed as the midpoint of its measurement interval.

Basal Area Curve Fitting

Three sets of curves were produced, per-acre basal area growth, per-acre basal area increment, and mean-tree basal area, for each plot in the data set. Cumulative and increment forms of the Richards model (Eq. 9a-b) were fit to the data along with cumulative and increment forms of the Schnute model (Eq. 10a-b). Regression was performed using the derivative-free nonlinear least squares regression procedure PROC NLIN found in SAS/STAT (SAS Institute Inc., Cary, N.C.) software. The BA_{rate} equations (Eq. 9b, 10b) used the ages at the midpoints of the growth intervals as values for the independent variable. Growth equations (9a, 10a) used the age at time of measurement.

$$BA = a\left[1 - e^{b(Age - A_o)}\right]^c \tag{9a}$$

$$BA_{rate} = -abc \bullet e^{b(Age - A_o)}\left[1 - e^{b(Age - A_o)}\right]^{[c-1]} \tag{b}$$

$$BA = \left[BA_1^{\frac{1}{c}} + \left(BA_2^{\frac{1}{c}} - BA_1^{\frac{1}{c}}\right)\frac{1 - e^{b(Age - Age_1)}}{1 - e^{b(Age_2 - Age_1)}}\right]^c \tag{10a}$$

$$BA_{rate} = -bc \bullet \frac{\left(BA_2^{\frac{1}{c}} - BA_1^{\frac{1}{c}}\right)e^{b(Age - Age_1)}}{1 - e^{b(Age_2 - Age_1)}}\left[BA_1^{\frac{1}{c}} + \left(BA_2^{\frac{1}{c}} - BA_1^{\frac{1}{c}}\right)\frac{1 - e^{b(Age - Age_1)}}{1 - e^{b(Age_2 - Age_1)}}\right]^{c-1} \tag{b}$$

where

Age_1 - Age of first measurement
Age_2 - Age of final measurement
BA_1 - Estimated basal area at Age_1

BA_2 - Estimated basal area at Age_2
a,b,c - Estimated parameters

Age of Culmination of Basal Area Growth

Culmination age was defined in Eq. (5) as $A^* = A_o + \frac{1}{b}\ln\left(\frac{1}{c}\right)$ for the Richards curve with parameters a, b, and c. The Schnute model culmination age is

$$A^* = T_1 + T_2 + \frac{1}{b}\ln\left[\frac{\frac{1}{c}(e^{[-bT_2]}y_2^{\frac{1}{c}} - e^{[-bT_1]}y_1^{\frac{1}{c}})}{y_2^{\frac{1}{c}} - y_1^{\frac{1}{c}}}\right]^c \qquad (11)$$

The values of A* were computed from the parameter estimates of each regression procedure.

Modeling Canopy Closure

The crown closure index described by Spurr (1960) is generally measured from aerial photography. Since aerial photographs of the spacing trials were not available, it was necessary to compute crown closure from ground-level crown measurements. Crown closure was computed by a process involving the mapping of crown data on a coordinate plane, tessellation of the plane into a regular grid, checking grid locations for coverage by individual or multiple tree crowns, and calculating canopy closure by summation. Several variations on the same basic method were developed and tested in order to determine their effectiveness.

Mapping Crown Data

Relative stem locations were known because of the regular spacing in the study plots. By choosing one corner of the plot to be the coordinate plane origin, x-y coordinate pairs for each stem were readily obtained. The coordinate origin was placed at the upper left-hand corner of the plot (Fig 2) adjacent to tree 1 for convenience. The first row in each plot consisted of trees 1-7, the second row consisted of trees 8-14, etc. so that, as in Fig. 2, rows are oriented horizontally. In the actual spacing-trial design, trees are numbered in a serpentine fashion, where the orders of trees 8-14 are the reverse those shown in Fig. 2. The same is true of trees 22-28 and 36-42. Transforming to the left-right ascending order presented here simplified the geometry of the plot map.

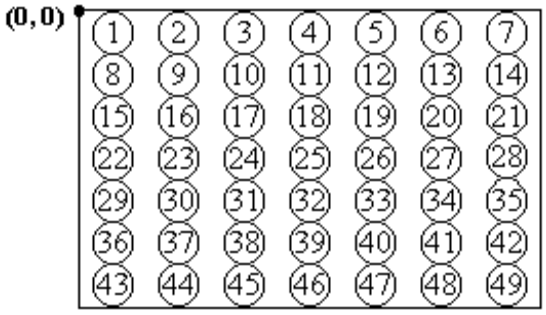

Figure 2. Arrangement of 49 trees on the plot map. Rows run horizontally so that the within-row distance (wrd) is the horizontal distance between column centers, and the between-row distance (brd) is the vertical distance between row centers.

The x and y-coordinates (x_c, y_c) for the center of tree n were obtained by

$$x_c = \text{wrd}\left(\text{mod}\left[\tfrac{n\text{-}1}{7}\right] + 0.5\right) \qquad (12a)$$

and

$$y_c = \text{-brd}\left(\text{int}\left[\tfrac{n\text{-}1}{7}\right] + 0.5\right) \qquad (b)$$

where

wrd - within-row distance
brd - between-row distance
mod - the modulo or remainder of division
int - the integer value, ignoring any decimal places

For example, tree 26 would have x and y coordinates (4.5 $\times$ wrd) and (-3.5 $\times$ brd), respectively, on the coordinate plane whose origin is located at the upper left-hand corner of the plot (Fig. 2).

Having established (x,y) coordinates for each measured stem, the individual trees' crowns were mapped around their stems. Because crown widths were measured in two directions – within and between rows – an elliptical crown shape was assumed. Based on this assumption, the perimeter of any tree's crown is given by set of points that satisfy the equation

$$\frac{(x - x_c)^2}{(\text{cww})^2} + \frac{(y - y_c)^2}{(\text{cwb})^2} = \frac{1}{4} \qquad (13)$$

where

x,y - x and y coordinates of the crown's perimeter
x_c,y_c - x and y coordinates of the crown center (stem)
cww - crown width within rows
cwb - crown width between rows

Tessellating the plot

Each plot was divided into a grid of equal-sized pixel-cells is so that each pixel could be checked versus its surrounding trees to determine whether it was covered by the projection(s) of any living crown(s). A pixel size relative to the plot area was used so that every plot − regardless of its size − could be divided into the same number of pixel-cells. Relative pixel area (p_{rel}) was chosen to be quite small, $p_{\text{rel}} = \frac{1}{112{,}896}$, effectively dividing each plot into $\frac{1}{p_{\text{rel}}} = 112{,}896$ pixel-cells. This p_{rel} by design corresponds to a regular grid comprised of 336 × 336 cells. The 336-cell grid system simplified working with plots whose dimensions were multiples of 7 trees and either 4, 6, 8, or 12 foot spacings. It also kept computation intensity to a manageable level. Under this equal-number, unequal-size grid system, pixel area is computed as $\frac{\text{plot area}}{112{,}896}$ so that pixels on the smallest plots represent 1 in^2 of land area and pixels on the largest plots represent 9 in^2. Pixel dimensions corresponding to the sixteen plot sizes in the spacing trial are listed in Table 2.

Table 2. Plot sizes and the corresponding pixel-grid sizes using a systematic grid of 336 × 336 = 112,896 pixels on each plot. The number of pixels is always constant, but pixel size varies from plot to plot.

Plot Number	Plot Spacing (wrd × brd)	Plot Area (ft^2)	Pixel Dimensions (x × y)	Pixel Area (in^2)
1	(4 × 4)	784	(1 × 1)	1
2	(4 × 6)	1176	(1 × 1.5)	1.5
3	(4 × 8)	1568	(1 × 2)	2
4	(4 × 12)	2352	(1 × 3)	3
5	(6 × 4)	1176	(1.5 × 1)	1.5
6	(6 × 6)	1764	(1.5 × 1.5)	2.25
7	(6 × 8)	2352	(1.5 × 2)	3
8	(6 × 12)	3528	(1.5 × 3)	4.5
9	(8 × 4)	1568	(2 × 1)	2
10	(8 × 6)	2352	(2 × 1.5)	3
11	(8 × 8)	3136	(2 × 2)	4
12	(8 × 12)	4704	(2 × 3)	6
13	(12 × 4)	2352	(3 × 1)	3
14	(12 × 6)	3528	(3 × 1.5)	4.5
15	(12 × 8)	4704	(3 × 2)	6
16	(12 × 12)	7056	(3 × 3)	9

Using formulae similar to Eqs. 12(a-b), which determine (x, y) coordinates for the center of any tree, it was possible to locate the center of any pixel p on the coordinate plane by its coordinates

$$x_p = pww\left(\mathrm{mod}\left[\frac{p-1}{336}\right] + 0.5\right) \quad (14a)$$

and

$$y_p = -pwb\left(\mathrm{int}\left[\frac{p-1}{336}\right] + 0.5\right) \quad (b)$$

where

pww - within-row pixel width
pwb - between-row pixel width

Checking for Coverage by Live Crowns

The information described in the preceding sections – stem location, crown perimeter, and pixel location – was used to check the pixels for coverage by live crowns. Each pixel was checked with the nearest trees to determine which was closer to the tree center – the pixel center or the crown perimeter. If the crown perimeter was closer to the tree center than the pixel center was, the pixel was considered "not covered" by that particular crown; otherwise, the pixel was considered "covered."

Each pixel was checked for coverage by the thirteen trees closest to it, including: the tree on whose growing space the pixel was situated, which was considered the "center tree"; two trees in each within-row and between-row direction of the center tree (total of eight); and one tree in each diagonal direction of the center tree (total of four). Every pixel was categorized into exactly one of four crown coverage categories: A) not covered; B) covered by one crown; C) covered by two crowns; or D) covered by three or more crowns.

The decision to check only the nearest thirteen trees was based partly on the observation that *only seventeen crown-width measurements in the data set exceed 3 times their plot's within-row or between-row spacing*. All seventeen were found to cover no other growing spaces than those of the surrounding thirteen trees; furthermore, they were all on non-square plots, and the excessive overlap was always in the direction of the narrow spacing. The vast majority of crown measurements (88,481) were narrower than 3 times their plot's within-row or between-row spacing. Under the elliptical shape assumption, such crowns will not overlap any trees' growing spaces except for those of their immediate neighbors.

Figure 3 shows the arrangement of trees that would be checked for crown coverage on a pixel that falls in the growing space of tree number 1. Tree number 1 is the center tree in this example. Its crown and those of the shaded trees around it were checked for coverage of the pixel. As the figure illustrates, crowns of the (non-measured) trees adjacent to the plot might contribute to crown coverage of pixels near the plot boundary. This effect, know as edge bias (Monserud and Ek 1974), was investigated in an attempt to compensate for it.

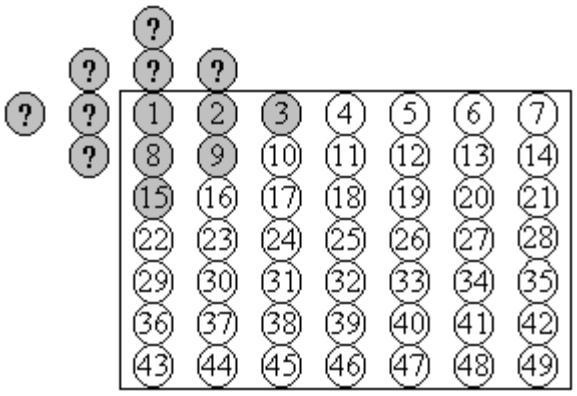

Figure 3. The arrangement of trees to be checked for live crown coverage of a pixel. The shaded trees would all be checked for coverage of any pixel in tree number one's growing space. Since trees outside the plot were not measured, "edge bias" may occur.

Edge Bias Compensation

Tests of the following edge-bias compensation algorithms were carried out on a reduced plot size of 5 by 5 trees:

1) Translation
2) Reflection via a reflecting line at the plot boundary
3) Reflection via a reflecting line through the edge trees
4) A random arrangement of interior trees around the plot.
5) No trees outside the plot

The random arrangement method essentially selected one tree at random (with-replacement) from the plot interior to occupy each tree position around the outside of the plot. Crown closure (CC) and crown overlap (CO) indices were computed for each method. CC was computed as the proportion of ground area covered by any live crown(s). CO was computed as the proportion of the ground area covered by at least two crowns. True CC and CO were computed from the 5 by 5 plots surrounded by the trees that were actually measured as a part of the full-sized 7 by 7 tree plots.

Results for all five methods were compared to the true values in the following manner. For each plot and measurement year, index error (E) was computed as the edge-bias corrected index value ($\hat{Z}$) minus the true index (Z). Relative error (E_{rel}) was computed as the ratio of E to Z. A full set of error data - 1912 observations - was generated for the CC and CO indices. The data set consisted of 192 plots each measured on 10 different occasions. Eight observations were missing as a result of ice-damage and insect infestation on some plots.

Two basic approaches were used to determine the relative accuracy of the methods. The first involved assuming an approximately normal distribution of E, and considering the data to be a sample from some hypothetical population of plots. This population would share the same distributional assumption and include the set of full-sized 7 by 7 plots. Any confidence, prediction, or tolerance interval widths are directly proportional to the standard deviation of E (Reynolds 1984), so the standard deviations serve as a measure of relative accuracy of the methods.

The second approach avoided the normal assumption and treated the 5 by 5 plot error data (N = 1912) as a complete population. The assumption was made, however, that the correction algorithms would generate a similar distribution of errors given the population of 7 by 7 plots as they did for the 5 by 5 population. Intervals over which ninety-five percent ($N_{95\%}$ = 1817) of the errors occurred were tabulated by removing the most extreme 2.5% of the observed E and E_{rel} from upper and lower ends of the distribution. These "incidence intervals" served roughly as an analogue to 95% prediction intervals and were used to compare model performance. By comparing the performance of the correction methods, a preferred method was chosen for implementation on the full plot.

Computing Crown Closure

The crown closure index (CC) was computed as one minus the proportion of all pixels "not covered" by any live crown projection. This is the index usually obtained from aerial photography, and its value is between zero and one. Three alternatives to the CC index were computed. The first was a crown overlap index (CO), computed as the proportion of the ground area covered by two or more crowns. Any pixel covered by two or more live crowns was counted in the numerator of this index. The CO index effectively ignores multiple overlapping areas of three or more crowns, tallying them only once. The second alternative - a multiple overlap (MO) index - computed overlap area without ignoring multiple overlap areas. A pixel covered by the live crowns of three separate trees, for example, would count as three pixels in the numerator. The third index - crown area projection (CAP) - was computed as the ratio of live crown projection area to plot ground area. The CAP index is nearly equivalent to the sum of all individual trees' crowns area projections divided by the plot area, except for the truncation of live crowns at the plot boundary. Technically, the CAP index could have been computed without employing any edge-bias correction, since crown areas of all on-plot trees were measured; however, the method of computation ensured that CAP equals the sum of CC, CO, and MO indices for a given plot.

The age of basal area culmination, A*, invariably was estimated to have taken place between measurement periods. Given the alternative of rounding culmination ages to the nearest integer, it was deemed reasonable to interpolate crown closure indices exactly to the point of A*. For each index, a value corresponding to the age A* was computed in this way for all 192 plots.

Crown Closure Relationships to Basal Area Growth

Graphical, tabular, and statistical methods were used to investigate trends between crown closure and the culmination of basal area increment. Where site differences were of interest, means were plotted and tested via regression analysis and the use of location indicator variables. Site index was computed as the mean height of the tallest 65% of trees on the plots, replicates, or locations of interest. Analyses similar to those that used indicator variables were carried out using site index.

Chapter 4
RESULTS

Edge-Bias Compensation

Table 3 compares the performance of the edge-bias correction algorithms:

1) Translation
2) Reflection via a reflecting line at the plot boundary
3) Reflection via a reflecting line through the edge trees
4) A random arrangement of interior trees around the plot.
5) No trees outside the plot

in estimating CC index. Methods 2 and 5 are clearly biased in that they are unable to overestimate CC, but frequently underestimate it. This result is reflected in the relatively large negative mean values for methods 2 and 5, and the upper boundary of their incidence intervals at zero. Methods 2 and 5 give identical results for the CC index as a result of their similar geometry. Methods 1, 3, and 4 perform nearly equivalently, with only small differences that do not promote an obvious distinction. Method 1, for instance, has a mean E closer to zero, but its individual errors are distributed over a wider range than either method 3 or 4. Relative errors for the CC index give results consistent with the results shown in Table 3 and are therefore not presented.

Table 3. Comparative statistics for five edge-bias correction algorithms, computed from 1912 error (E) terms, where E is the difference between edge-bias corrected and actual CC index.

Method	Mean	Std. Dev.	ΣE^2	95% Incidence Interval
1	-0.000314331	0.0054052	0.0560206	[-0.0134, 0.0092]
2	-0.0056187	0.0081654	0.1877748	[-0.028, 0.0]
3	-0.000414278	0.0051901	0.0518050	[-0.0116, 0.0094]
4	-0.000353033	0.0050583	0.0491337	[-0.0126, 0.0096]
5	-0.0056187	0.0081654	0.1877748	[-0.028, 0.0]

Table 4 compares the performance of the edge-bias correction algorithms in estimating crown overlap (CO) for the population of plot-years where any crown overlapping occurred (N = 1457). Here, relative errors (E_{rel}) are reported in the lower half of the table. As with the CC index, method 4 performs relatively well as judged by the collection of E terms; however, the observed E_{rel} values indicate a possible weakness in method 4 for estimating CO. Note that the standard deviation and sum of E_{rel}^2 values are considerably larger for method 4 than the other methods. This discrepancy was eliminated after removing the extreme upper and lower values ($N_{95\%}$ = 1385). Further investigation showed a small collection of extreme data whose E_{rel} ranged between 4 and 8 (i.e. 400 and 800 percent). These same observations had small absolute errors, but since they occurred on plots with small actual CO, the resulting E_{rel} was large.

Table 4. Comparative statistics for three edge-bias correction algorithms computed from 1457 error (E) and relative error (E_{rel}) terms, where E is the difference between edge-bias corrected and actual CO index values.

Method	Mean	Std. Dev.	ΣE^2	95% Incidence Interval
1 (E)	-0.00108	0.015416	0.347747	[-0.0363, 0.0324]
3 (E)	-0.00186	0.014797	0.323806	[-0.0352, 0.0284]
4 (E)	-0.00052	0.013185	0.253515	[-0.0298, 0.0275]
1 (E_{rel})	-0.01556	0.185868	50.65296	[-0.3378, 0.2522]
3 (E_{rel})	-0.02559	0.181478	48.9062	[-0.4257, 0.2379]
4 (E_{rel})	0.001986	0.309086	139.1038	[-0.3592, 0.3208]

Basal Area Curve Fitting

Initially, fits of the Richards model were unobtainable for some plots at the upper piedmont site since the fitting procedures failed to converge on a solution. These plots were also fitted to the Schnute model and, in most cases either failed to converge or converged to non-sigmoidal solutions. Graphs of these data revealed sharp decreases in basal area after age eleven followed by subsequent increases at age twelve. The decreases were caused by mortality during the twelfth growing season due to ice damage from the previous winter. Plots numbered 1, 2, 5, 6, 10, 12, 13, and 15 on the second replicate, and plots 8 and 9 on the third replicate were found to have suffered damage to at least ten percent of their trees. The damage resulted in a basal area decrease between ages 11 and 12 on each of these plots, with the exception of plot 5 on the second replicate; however, the basal area on plot 5 was clearly affected by the ice damage. Basal area observations for ages 12 and 13 on these plots were removed from the data to facilitate the estimation of the curves' inflection points.

Basal Area per Acre

After having removed the data affected by catastrophic mortality, the models were fit to basal area per acre data and gave results which were sensible; however, curve fits on certain plots gave conflicting parameter estimates. Of the 192 plots fitted to the basal area per acre models, 177 gave estimated culmination ages within 0.01 percent of each other. For these plots, Richards and Schnute curve shape parameters (b and c) were identical except for some small differences assumed to be associated with numerical rounding. Figure 4 illustrates the result that most of the culmination age estimates are identical for the Richards and Schnute models, i.e. they fall along the line of slope 1 when plotted against each other. The same result is shown for b and c parameter estimates, which are the component variables that determine culmination age.

As noted above, the 15 plots that generated conflicting estimates of the b and c parameters also yielded conflicting estimates of culmination age (Fig. 4). Besides the critical difference of at least 0.01% in estimated culmination age, another significant difference was

found: For all 117 compatible estimates, the estimate of the Schnute parameter y_1 was exactly zero, but for the plots which gave conflicting estimates, y_1 was estimated as a positive number ranging from 0.0019 to 0.84 square feet per acre. These positive estimates of y_1 seemed illogical when interpreted as the basal area of the plot at A_o, the age when the first tree on the plot reaches breast height.

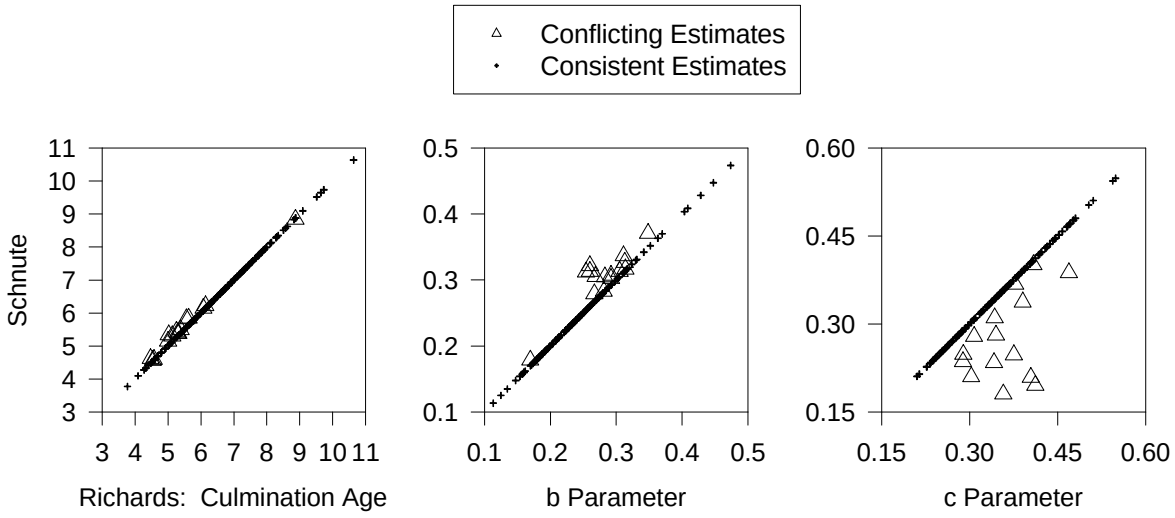

Figure 4. Schnute versus Richards estimates for the culmination age of basal area per acre, and parameters b and c for growth curves on 192 experimental plots. The 15 plots whose culmination age estimates differed by more than 0.01% are labeled as conflicting estimates.

It was noted that the Richards formulation (Eq. 9) makes full use of derived A_o information, fixing A_o rather than estimating it as a parameter. The Schnute formulation, however, uses known information about A_o but ignores known (derived) information about the initial size. Namely, initial basal area is zero at A_o, so it should be reasonable to fix $y_1=0$ rather than estimate it from the data. Furthermore, sums of squared-errors were nearly identical for four-parameter Schnute and three-parameter Richards model fits, which resulted in systematically higher mean squared-error (MSE) values for the Schnute model. Thus, fitting the additional parameter was deemed superfluous. Proceeding with this reasoning, y_1 was fixed at zero in the Schnute model, and a simpler three-parameter model was constructed (Eq. 15). It's first derivative with respect to age, or increment form, is given by Eq. 16.

$$BA = y_2 \left[\frac{1 - e^{b\,(Age - T_1)}}{1 - e^{b\,(T_2 - T_1)}} \right]^c \tag{15}$$

$$\frac{\partial\, BA}{\partial\, Age} = \frac{-bc\, y_2 e^{b\,(Age - T_1)}}{1 - e^{b\,(T_2 - T_1)}} \left[\frac{1 - e^{b\,(Age - T_1)}}{1 - e^{b\,(T_2 - T_1)}} \right]^{(c-1)} \tag{16}$$

Parameter and culmination age estimates from the modified Schnute model (Eq 15) were equivalent to the Richards parameter estimates for all 192 plots, with some minuscule differences

probably attributable to rounding error. Sums of squared-errors and MSE statistics consequently achieved the same equivalence.

When increment data were fitted to the first derivatives of the Richards model (Eq. 9b) and the modified Schnute model (Eq. 16), parameter estimates, culmination ages, and MSE results were indistinguishable. The increment fits furnished a full set of parameter estimates with which to compare to the parameter estimates from the cumulative growth fits.

Figure 5 shows a comparison of culmination age and parameter (b and c) estimates for the growth versus increment data. Culmination ages do not lie exactly along the line of slope equal to one, indicating that there is some variation between the values estimated from growth and increment data. The magnitude of this variation is relatively small. The culmination age is on average about 0.75 percent larger when fitted to growth data than when fitted to increment data. The largest difference was about 9.2% and the smallest was -2.4 %. When the variation of the component parameters (b and c) is studied, one sees that the magnitudes of variation are considerably larger. Parameter b estimates vary by anywhere between -20 and +16 percent. Parameter c estimates vary by as much as -30 and +8 percent. Negative values indicate that the estimates from growth data are smaller than the estimates from the corresponding increment data.

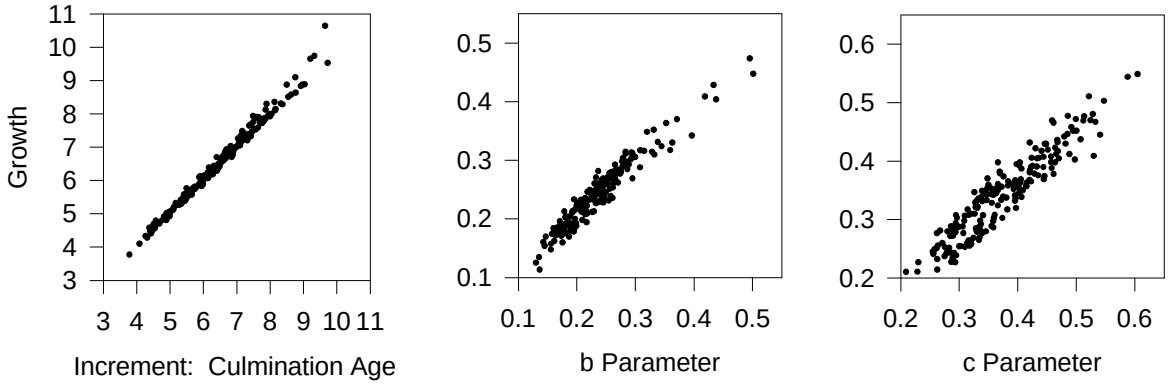

Figure 5. Comparisons of estimated basal area culmination age, and parameters b and c for growth versus increment curve fitting.

Consideration was given as to which set of parameter estimates was preferable. Mean squared-error statistics could not be compared between the growth and increment models since the responses did not share common units of measure (square feet as opposed to square feet per year). Fit statistics were typically better for the growth models than their increment counterparts, however. Adjusted R^2, computed as $1 - \frac{\text{MSE}}{\text{MS(corrected total)}}$ (Sit and Poulin-Costello 1994), commonly ranged above 0.95 for the growth fits and below 0.85 for the increment fits. Every increment data set sacrificed exactly one observation compared to its corresponding growth data set; thus the growth models always had one additional degree of freedom.

Quadratic Mean Diameter

Quadratic mean diameter, or the diameter of the mean-tree basal area, was computed as QMD = $\sqrt{\frac{BA}{N\ (0.005454154)}}$, where N is the number of surviving trees per acre taller than breast height. Fitting QMD data to the Richards model gave culmination age (A^*_{QMD})estimates considerably smaller than the per acre basal area culmination age estimates; however, it was determined that these estimates were smaller only because of the effect of the power transformation of the basal area data. When A^*_{QMD} estimates were corrected for the power transformation, they became equal to or larger than the per acre A* estimates. (The correction involved working with mean-tree basal area $\overline{BA}$ rather than mean-tree diameter - see Appendix A). Of 192 estimated $A^*_{\overline{BA}}$ values, 78 were nearly equivalent to their corresponding estimated A*, but 114 exceeded A* by at least 0.1 year.

Some of these differences could be attributed to mortality that occurred at relatively late ages. Such mortality elevated $\overline{BA}$ at these late ages. For example, 19 plots had at least 10 percent mortality by age 10. This type of mortality was the exception rather than the rule, however. Seven-tenths of all plots on the spacing trials had 96% or better survival at age 10.

The other identified cause of inflated $A^*_{\overline{BA}}$ estimates involved the earliest stages of basal area development. For ages before five years, it was commonly found that some fraction of trees had not yet reached breast height For example, 130 plots had fewer than half of their planted trees taller than 4.5 feet at one or more measurement cycles prior to age 5. Because of this "recruitment" effect and the aforementioned impact of mortality, further analyses relied on culmination ages estimated only from per acre basal area data.

Site Index

Mean heights of the tallest 65% (5158) of undamaged trees (7934) were tabulated by location for use in a dominant-codominant height site index equation. Mean heights were significantly different for all locations when only location was accounted for. A regression analysis was performed using indicator variables to determine mean height of dominant and codominant trees (HD) for all locations locations and establish the significance of the mean differences (all $p \leq 0.0001$).

$$HD = 32.00 + 4.898(z_1) - 0.694(z_2) + 1.188(z_3) \quad (17)$$

where

HD - mean height (ft) at age 12 for 65% of tallest trees at each location
z_1 - 1 for upper Piedmont, 0 otherwise
z_2 - 1 for lower Piedmont, 0 otherwise
z_3 - 1 for upper Coastal Plain, 0 otherwise

In a supplementary analysis, all twelve replicates had significantly different mean HD; furthermore, significant effects of spacing on mean height were found throughout the study. To avoid confounding site and spacing variables in further analyses, trees were finally grouped by location only, and the tallest 65% were selected from each location for site index determination. The results of the grouping by location are shown in Table 5. Site index (SI) was predicted from the dominant height curve developed by Amateis et al. (1995).

Table 5. Age 12 mean height and estimated site index of tallest 65% of trees by location. Site index is computed for base age 25.

Location	Mean Height (ft)	Site Index
Upper Piedmont	36.9	64
Lower Piedmont	31.3	53
Upper Coastal Plain	33.2	56
Lower Coastal Plain	32.0	54

Culmination Ages

Culmination ages varied by site as well as spacing. The upper Piedmont and Coastal Plain sites generally reached basal area culmination at younger ages than their lower counterparts. Plots with narrower spacing reached basal area culmination at younger ages than widely spaced plots. Figure 6 shows the mean culmination age by growing space for all four sites in the spacing trials. Plots with identical growing space, regardless of spacing (e.g. 4' $\times$ 12' and 6' $\times$ 8'), were combined from all three replicates at each location to compute the mean values. Upper and lower Piedmont sites are shown in the left-hand scatterplot and Coastal Plain sites are shown on the right. Average growing space per tree ranges from 16 square feet on the most narrowly-spaced plots to 144 square feet for the most widely-spaced.

A multiple linear regression was performed on culmination age versus growing space for all 192 plots, with indicator variables used to distinguish between study locations (Figure 6). The regression showed that the effect of spacing was significant to the model (p=0.0001). Location significantly altered the model intercept from the base intercept given by the lower Coastal Plain model (p_{UCP}=0.0001; p_{LCP}=0.0001; p_{LP}=0.0002). Further linear regression analyses showed that some interactions between location and spacing may also be significant.

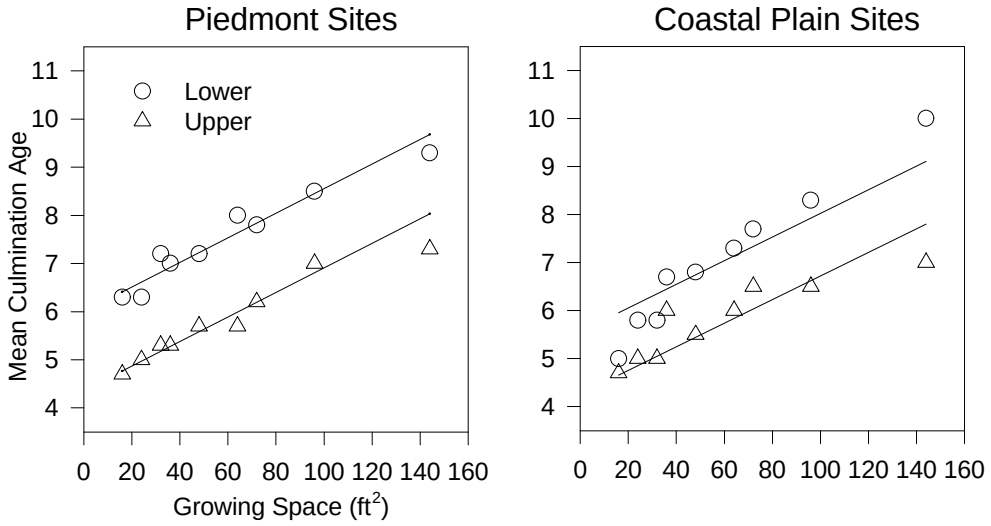

Figure 6. Mean basal area culmination age by growing space for experimental plots located in the upper and lower Piedmont and Coastal Plain physiographic regions. Regressions lines showing the effects of spacing and location on culmination age (Eq. 19) are superimposed.

Site index was found to adequately detect the differences found in mean culmination age between the various study locations. In the regression

$$A^* = 11.85 + 0.0247(GS) - 0.1194(SI) \quad (18)$$

where

GS - average growing space (ft^2) per tree planted
SI - Site index (ft, base age 25 years)

all terms were significant to the model (all $p \leq 0.0001$), despite the relatively high percentage of unexplained variability (r^2=0.581). Site index values from Table 5 were used in fitting Eq. (18). A model which used location indicator variables rather than SI fit the data more closely (r^2= 0.767).

$$A^* = 5.564 + 0.0246(GS) - 1.119z_1 + 0.477z_2 - 1.304z_3 \quad (19)$$

Crown Closure

Plots on the upper Piedmont site having suffered significant ice damage as described in the results of basal area curve fitting were removed from the analysis. Additionally, plots numbered 4 and 11 from the first replicate and 11, 12, and 15 from the third replicate were excluded from the crown closure analysis. These plots showed evidence of mortality or missing observations and, in all cases, at least 20% of those plots' crowns showed visible damage at the 12-year remeasurement. Trends in canopy closure and its relationship to culmination age were evident in spite of the loss of these data.

The four appraised crown closure indices generally exhibited an initial stage of monotonic increase to some maximum level of crown closure (Fig. 7). The age at which the 4' × 4' plots reached maximum crown closure was also the point of greatest difference between crown closure from the widest to narrowest spacings. On narrowly-spaced plots, crown closure typically decreased to some lower level after reaching its maximum. The widely-spaced plots, however, followed a generally uninterrupted upward trend in crown closure through age 12. The net result showed crown closure for all spacings roughly converging to the same level by age 12. Mean CC values for upper and lower Piedmont, and upper and lower Coastal Plain sites (standard deviations in parentheses) at age 12 were .74 (.27), .91 (.07), .87 (.06), and .85 (.11), respectively.

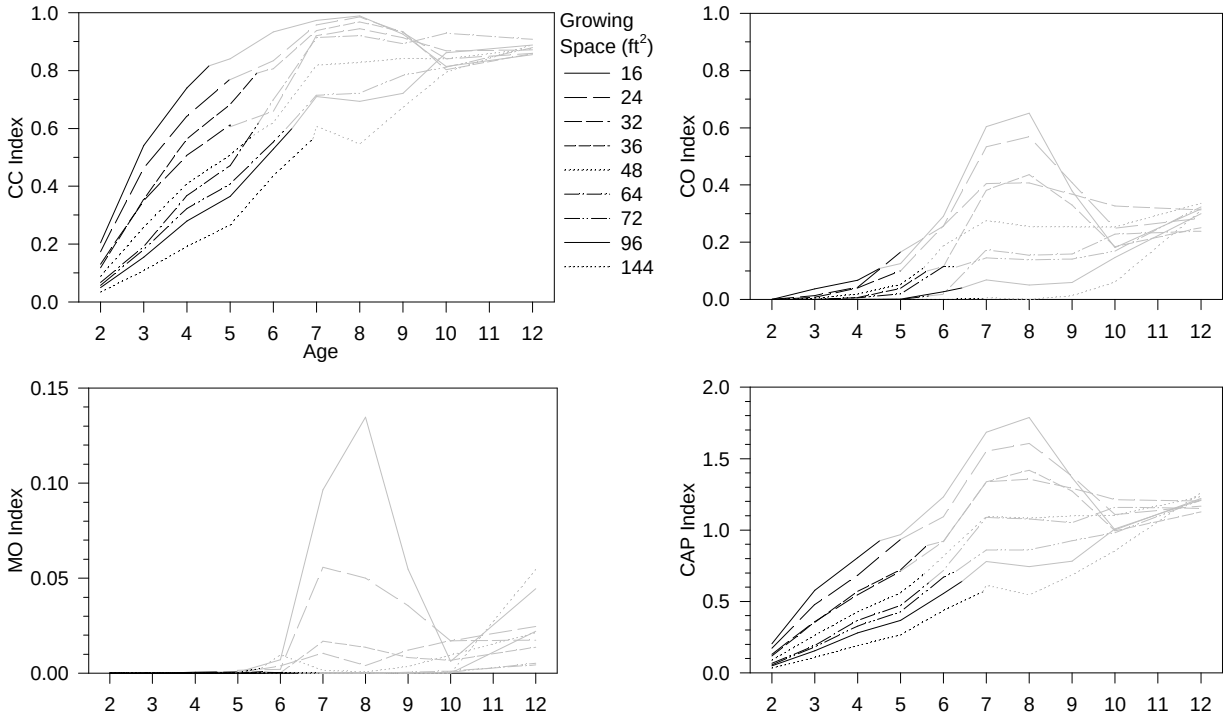

Figure 6. Mean crown closure indices - CC, CO, MO, and CAP - by age (years since planting) and growing space (ft^2) for plots on the upper Coastal Plain. Curves are shaded dark before the culmination age and light after it. No measurements were taken at age 11.

Figure 7 shows the mean CC, CO, MO, and CAP indices by age and growing space for plots on the upper Coastal Plain site. The trends described above are evident in the figure, and are also evident in similar plots made for the other locations but not presented here. The crown overlap plot in Figure 7 (upper right-hand plot) reveals some time-correlated variation in the rates of crown overlap change, i.e. the rates of CO change seem to speed up and slow down at roughly the same time, regardless of spacing. At this site, CO tended to decrease or stay the same between ages 8 and 9, regardless of spacing. The same trend was evident on plots of the Piedmont sites. There, CO decreased sharply for nearly every curve between ages 8 and 9.

Crown closure indices prior to the age of basal area culmination consist almost entirely of the monotonically increasing portions of the crown closure curves illustrated in Fig. 7 (dark shading). The MO index shows virtually no multiple overlapping prior to the culmination age. Note that the vertical scale of the MO index is amplified and the CAP index vertical scale is muted. The CAP index is effectively the sum of the other three curves.

A regression of pre-culmination-age CC versus Age, SI, and GS showed significant interaction between GS and Age, and fit the data well (r^2=0.796). The fitted model shows significance of all its terms (all $p \leq 0.0001$).

$$CC = -1.062 + 0.160(Age) + - 0.00131 + 0.0171(SI) - 0.000470(GS \times Age) \quad (20)$$

where

Age - Years since planting

Crown Closure at Basal Area Culmination Age

When crown closure at culmination age (CC*, CO*, etc.) is plotted versus growing space, a clear functional relationship is noted (Figure 8). The data plotted in Figure 8 correspond to the points of transition from dark to light shading in Figure 7, but raw data are presented here rather than mean CC* or CO*. Differences between locations are not as obvious as the trends due to spacing. Regressions of CC* on GS and site variables were fitted, using alternative models (Eq. 21-22).

$$Index^* = b_o + b_1(GS) + b_2 z_1 + b_3 z_2 + b_3 z_3 \quad (21)$$

$$Index^* = b_o + b_1(GS) + b_2(SI) \quad (22)$$

where

Index*-various crown closure indices (CC, CO, MO, CAP) at age A*

b_o-b_4 - fitted parameters

The results of fitting parameters in Eqs. (21-22) to the crown closure indices for all 192 plot observations are listed in Table 6. P-values for the parameter estimates are all 0.0001 unless shown in parenthesis. The parameter estimates on the growing-space term (b_1) were always significant to either model. Regression fits were always better using indicator variables (Eq. 21) than they were for the site index formulation (Eq. 22). The CAP* models outperformed the CC*, CO*, and MO* models, both in terms of fit and significance of the parameters.

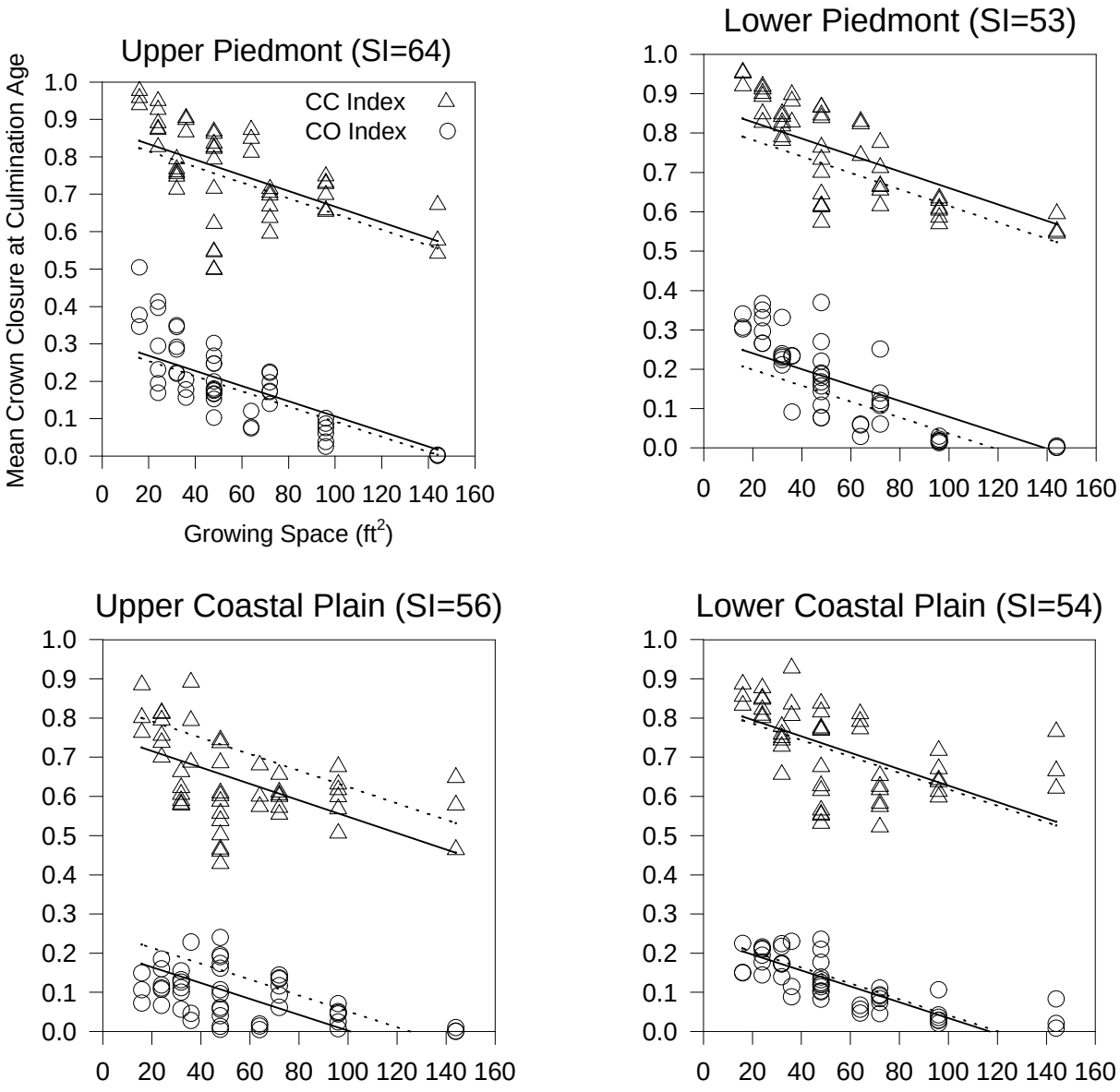

Figure 8. Crown closure at the age of basal area culmination for crown closure and crown overlap indices (CC* and CO*) by growing space and location. Site index (ft, base age 25) was computed from mean heights of the 65% tallest trees at each location, using the equation of Amateis et al. (1995). Regression lines fit to 48 plots per location are superimposed. The regression using location indicator variables (Eq. 21 - solid lines) is contrasted to one using site index (Eq. 22 - dashed lines).

Table 6. Parameter estimates for multiple linear regressions of three crown closure indices on growing space and location. The top half of the table shows estimates for Eq. (21), which uses location indicator variables. The bottom half shows estimates for Eq. (22), which uses site index. P-values not shown (parentheses) are < 0.001.

Index	r^2	b_o	b_1	b_2	b_3	b_4
CC*	0.432	0.8371	-0.0021	0.0394 (0.047)	0.0333 (0.092)	-0.0792
CO*	0.589	0.2367	-0.0020	0.0716	0.0446 (0.001)	-0.0320 (0.018)
MO*	0.114	0.0034 (0.017)	-0.0001 (0.002)	0.0050 (0.001)	0.0031 (0.043)	0.0004 (0.774)
CAP*	0.651	1.077	-0.0042	0.1161	0.0812 (0.001)	-0.1107
CC*	0.302	0.6685	-0.0021	0.0029 (0.099)	none	none
CO*	0.478	-0.0277 (0.693)	-0.0020	0.0050	none	none
MO*	0.079	-0.0127 (0.083)	-0.0001 (0.002)	0.0003 (0.012)	none	none
CAP*	0.493	0.6284	-0.0042	0.0083 (0.001)	none	none

Observable multiple crown overlapping was quite rare on pre-culmination age plots. Of 995 plot measurements prior to culmination ages, only 46 yielded nonzero computed MO index. Exactly 5 of these values were greater than 1% (0.01), which could be considered a minimum observable MO. The mean MO of these five observations was just 2.9%. A query of the interpolated MO* index showed 83 plots with nonzero multiple overlap at age A*. All but twelve of these plots had less than 1% (interpolated) multiple overlap (MO* = 0.01), and the mean value of the twelve that did have greater than 1% multiple overlap was just 2.8%. There was one instance where multiple overlap exceeding 1% preceded A* by 1.06 years; otherwise, "observable" MO values ($\geq$ 0.01), occurred no earlier than the measurement period immediately prior to basal area culmination age.

Effects of Rectangularity

Figure 8 and similar scatterplots of MO* and CAP* show that for square spacings, GS = {16, 36, 64, 144}, within-location variability is relatively low; furthermore, the greatest variability generally occurs at GS = 48, which consists of 6' $\times$ 8' and 4' $\times$ 12' spacings. These extremes in rectangularity cause a great deal of the variability in CC* and MO* at GS = 48. For example, in the Upper Piedmont scatterplot (Fig. 8), all 6' $\times$ 8' plot CC* observations (GS=48, $\triangle$) lie above the solid regression line and all of the 4' $\times$ 12' plots fall below it. The converse is true for the CO index, that is, the larger CO* values at GS=48 belong to 4' $\times$ 12' plots. A similar result is found at all four locations, namely, the extremely rectangular 4' $\times$ 12' plots have lower crown closure but higher crown overlapping at A* than their more squarely-spaced counterparts.

Results of regressions fitting Eqs. (21-22) with only square spacings are listed in Table 7. As with the full data set regressions, Eq. (21) fits the data better than Eq. (22). All indices but the crown overlap index (CO*) show an improved fit to these linear models when rectangular spacings are removed. The CC* model shows better fit to the data and more meaningful parameter estimates of b_o and b_1 than the other indices. Whereas the effect of location -

especially site index - was somewhat unclear for the full data set, its effect is consistently insignificant for square spacings.

Table 7. Parameter estimates for multiple linear regressions of three crown closure indices on growing space and location (square spacings only). The top half of the table shows estimates for Eq. (21), which uses location indicator variables. The bottom half shows estimates for Eq. (22), which uses site index. P-values not shown (parentheses) are < 0.001.

Index	r^2	b_o	b_1	b_2	b_3	b_4
CC*	0.809	0.9461	-0.0023	0.0249 (0.333)	-0.0041 (0.873)	-0.1003
CO*	0.592	0.2124	-0.0017	0.0667 (0.049)	0.0351 (0.293)	-0.0467 (0.164)
MO*	0.166	0.0040 (0.173)	-0.0001 (0.040)	0.0057 (0.094)	0.0025 (0.467)	0.0002 (0.956)
CAP*	0.755	1.163	-0.0040	0.0976 (0.072)	0.0336 (0.529)	-0.1472 (0.008)
CC*	0.697	0.7207	-0.0023	0.0036 (0.164)	none	none
CO*	0.503	-0.0678 (0.686)	-0.0017	0.0052 (0.082)	none	none
MO*	0.136	-0.0188 (0.236)	-0.0001 (0.039)	0.0004 (0.118)	none	none
CAP*	0.650	0.6331 (0.034)	-0.0040	0.0093 (0.074)	none	none

Rectangularity effects on culmination age were not as apparent as its effects on crown closure. Visual inspection of the A* versus spacing plots separated into square and rectangular categories showed no obvious differences. A regression of A* on growing space and site index, using only plots with square spacing, gave the following fitted equation.

$$A^* = 12.26 + 0.0234(GS) - 0.1274(SI) \qquad (23)$$

This equation explains more of the variability in the data (r^2=0.671), which indicates an improvement over the full data-set model (Eq. 18). For typical sites ($55 \leq SI \leq 60$), the square-spacing model (23) predicts culmination ages higher than (Eq. 18) in the range of 0.1 to 0.3 years.

Predicting the Culmination Age of Basal Area Increment

Prediction of A* from existing (pre-culmination-age) stand conditions can be accomplished in either of the following two ways. First, where good estimates of site index are available Eq. (18) can be applied directly. From A* the number of years until culmination age (ΔA) is computed as $\Delta A = A^* - Age$ ($A^* \geq Age$).

An alternative model makes use of the CC versus Age relationship described by Eq. (20). The slope of Eq. (20) or a similar CC curve with respect to age is, in general $m = \frac{\Delta CC}{\Delta Age}$. For an observed CC_i at some pre-culmination age (A_i) and the unknown CC* at age A*, the slope formula becomes $\frac{CC^* - CC_i}{A^* - A_i}$, which can be written as $\Delta A = \frac{CC^* - CC_i}{m}$. The CC* can be predicted from a simple linear model of CC* on growing space, $CC^* = a + b(GS)$, based on Eq. (22) and the lack of evidence of a significant site index effect on CC*. The slope term m can be derived

from any terms in a model like Eq. (20) that involve Age. Using the Eq. (20) model form as a starting point, the prediction equation was formulated as

$$\Delta A_i = \frac{a + b(GS) - CC_i}{c + d(GS)} \quad (24)$$

where

ΔA_i Time (years) between age i and A* - the culmination age of BA increment
GS Average growing space per tree (ft^2) at planting density
CC_i Crown closure ratio observed at some age i
a - d estimated parameters

Rather that substitute parameters estimated from models (22) and (20) in the numerator and denominator of model (24), non-linear regression to estimate the parameters simultaneously was carried out. Starting values of the parameters were determined from individual (linear) regressions of the components (CC* and m) of the model. The model was fit to square-spaced plot data only to avoid the effects of rectangularity on crown closure. Results of the regression (standard errors in parentheses) are shown in Table 8.

Given that dominant/codominant height information may be available as an input to this type of model, it was augmented to

$$\Delta A_i = \frac{a - CC_i}{c + d(GS) + e(HD_i)} \quad (25)$$

where

HD_i Average height (ft) of the tallest 65% of trees on the plot at age i
e estimated parameter

and all other variables are as listed in Eq. (25). The GS term in the numerator of Eq. (25) was removed because the Asymptotic 95% confidence interval output of SAS PROC NLIN covered the origin. This model was also fit to the square-spaced plot data, and the results of estimation are given in Table 8. Comparison of mean-squared error statistics (Table 8) shows that Model 25 is a more accurate predictor of ΔA.

Table 8. Regression parameter estimates for ΔA prediction models Eqs. (24-25). Mean-squared errors for the models were 0.561 and 0.423, respectively.

Parameter	Model (24)	Model (25)
a	1.0515 (0.0363)	1.0893 (0.0487)
b	-0.00306 (0.000294)	
c	0.2533 (0.0134)	0.2243 (0.0135)
d	-0.00106 (0.00010)	-0.00076 (0.00008)
e		0.0142 (0.00171)

The ΔA model is applicable only when the existing stand has not yet reached culmination of BA increment, which requires some determination of a stand's A*. Eq. (18) can be used to make such a determination, but some estimate of site index will be needed; however, even rough ($\pm$ 10 ft) estimates of SI will give some practical information on how close the stand is to its culmination age. Once it has been determined that a stand has not obviously passed age A*, Eq. (26), a regression of CC* versus growing space fit to the square-spaced plots,

$$CC^* = 0.926 - 0.00229(GS) \qquad (26)$$

can be applied to confirm the determination of pre- or post-culmination-age conditions. Any observed CC higher than the model's predicted CC* for the age of observation signals that use of the ΔA model would not be appropriate.

Chapter 5

DISCUSSION

Edge-Bias Compensation

As Ek and Monserud (1974) noted, edge bias should generally not be ignored, especially when study trees are near the plot edge or interior trees are large enough to interact with others outside the plot boundary. These conditions would be favored by relatively old stands of large trees, small plot sizes, and spacing narrow enough to place some trees very close to the plot boundary. The error in edge bias correction algorithms increases with these same conditions as well, but the magnitude of error was small for this application. However, some clear disadvantages were observed when reflection by a line through the edge tree was compared with the other three compensation algorithms.

Methods 1, 3, and 4 performed comparatively in predicting CC and CO indices. The random arrangement (method 4) showed the only erratic behavior of the three, based on the few extreme relative errors it generated for the CO index. With this exception, random arrangement showed promise as a method of correcting for crown closure edge-bias with as much accuracy as either translation or reflection.

Reflection and translation performed nearly equally as well. The only consistent differences between the two were that translation yielded mean errors closer to zero in every test performed, while reflection always had the lower standard deviation of the two. Incidence intervals gave mixed results, depending on the index and choice of scale - relative or absolute. The apparently inflated negative bias of mean error terms for the reflection algorithm may be related to the nature of the algorithm itself. It might be unreasonable to expect that a constructed plot edge with identical trees on two sides of border trees mimics reality. Reflection is nothing more than a mirroring of trees to a location two trees away. Translation accomplishes the same task, but that the target location is further away (in this application, 5 trees) from the subject tree. Perhaps an intermediate distance (e.g. 3 or 4 trees) would produce better results than either method tested here.

Reflection was chosen for application on the 7×7 plots for the crown closure analyses in this study. It gave more precise estimates of CC and CO than translation on the 5×5 plot simulation, the magnitude of its mean error term was virtually undetectable in terms of actual crown closure, and it avoided extreme relative errors for the CO index, unlike the random arrangement method.

Basal Area Curve Fitting

The solution of fixing the Schnute model parameter y_1 at zero was not difficult to implement once the problem was discovered. The statistical implications of fixing Richards A_o or Schnute y_1 parameters at zero, however, are somewhat unclear to me. A certain advantage is that one degree of freedom is spared when the model is anchored to zero at the initial age. The loss in flexibility of the model is not unwarranted, since we have good information about the onset of basal area accumulation. The encounter did point out a minor weakness of the Schnute model in this application, however. Namely, estimation of parameters near zero (or in this case, expected to be zero), can be problematic. The SAS PROC NLIN gave ample error messages as iterations attempted to test negative values of y_1 to a fractional power ($\frac{1}{c}$). Furthermore, numerical problems with near-singularity of the Jacobian were often reported. It was suggested to me that estimating parameters of largely different magnitude can also lead to such numerical difficulties. Possible solutions might have included scaling the data so that the parameters would converge on more manageable solutions. Because the modified, three parameter Schnute model worked adequately, this solution was not implemented.

Site Index

The decision to assign a common site index value to all replicates at a particular location was perhaps inappropriate, given that all replicates had significantly different mean HD. Although this was the case, it is unlikely that these replicates would be placed into distinct stands (i.e. distinct site index classification) in the standard practice of forestry. Although small differences between within-site replicates were ignored, an effort was made to avert the problem of spacing effects on dominant-tree height growth. This problem, when ignored, likely poses a greater threat to the accuracy of forest growth models than the issue of within-stand height-growth variability. In any case, site index was used to distinguish between study locations of distinctly different character, and in that sense, it was applied correctly. The problems associated with comparing basal area culmination and crown closure based on a site index supersede this single issue, however. One particular concern is the poor extent to which site index is correlated with the various early-stand basal area and crown measures examined in the study. The lack of efficacy in using site index as a predictor of culmination age illustrates the point.

Site index is well correlated with the heights of dominant and codominant trees at age 12 (Table 5, $\rho = 0.997$), because it is predicted directly from the observed dominant/codominant height data. As such, it will indicate cumulative height growth potential of the study locations at that age. Unfortunately, mean dominant height at age 12 is not equally well-correlated with location mean $\overline{A^*}$ ($\rho = -0.738$). This relative weakness of the $\overline{HD}$ to $\overline{A^*}$ linear relationship means that formulating the linear regression of A* in terms of SI will always be less powerful than using site indicator variables. Thus, the regression fitted in Eq. (18) explains less of the variability in A*, even though it has attempted to account for the same growing space and site differences explained by Eq. (19). The gain is that site index is a quantitative indicator of site

quality, and can be applied to data other than the study population, whereas indicator variables cannot.

Further gains can potentially be made by finding a stronger relationship between $\overline{HD}$ and $\overline{A^*}$ other than the simplified linear assumption made here. The assumption was made to demonstrate the point that a relationship exists, not necessarily to find the exact nature of that relationship. The same principle motivated the use of linear regression tools in many of the analyses performed, and will be discussed further in the following section.

Culmination Ages

As noted, the assumption of linearity used to test significance of spacing and location effects on culmination age (Fig. 6) was somewhat of an oversimplification of the response. The fitted model (Eq. 19), if correctly specified, illogically implies that as planting density goes to infinity ($GS \rightarrow 0$), culmination will occur between 4.3 and 6.0 years after planting, depending on the study location. Moreover, culmination age is not bounded by any upper limit for open grown stands.

A deductive approach might be taken to improve the A* versus GS model. For instance, a reasonable assumption may be that there is some extreme density of planting that will accelerate competition to the point where culmination occurs exactly at A_o, the age at which the first tree in the stand reaches breast height. It is interesting to note that, under this condition, basal area growth would no longer follow a sigmoidal trend, but a strictly asymptotic one. This was the trend found by Bredenkamp and Gregoire (1988) in data from the median of their spacing trial data. At wider spacings, culmination age would occur at later ages, until the growing space was increased to the open-grown condition. There, culmination age would reach some maximum value which would not increase with further decreases in density. Various functions could be used to approximate this model and likely surpass the fit and explanatory power of the multiple linear model (Eq. 19).

Basal area culmination age estimates do not necessarily signal the onset of competition within the spacing trial plots. For instance, the power relationship between basal area and diameter ensures that basal area estimates of A* will be systematically higher than estimates derived from diameter data (see Appendix A). A possible interpretation of this condition is that culmination of diameter growth would serve as an earlier indicator of competition effects on stem growth. Nevertheless, A* estimates provide a measure of the age beyond which competition unequivocally reduces the rate of per acre basal area growth. This could be considered an appropriate (conservative) estimate of the onset of competition. The possible exception may be found in open-grown stands, whose basal area increment presumably culminates in the absence of competition.

Evidence of earlier competitive effects could be derived from the data in a number of ways, including the intersection-of-mean-diameter-curves approach taken by Strub et al. (1975).

Alternatively, a model could be designed that is flexible to allow growth trajectories that vary with initial spacing. All mean-diameters would be zero at the same site-corrected initial age. Over time, diameter curves for various spacings would diverge. Differences in curve slopes at a point in time would indicate the relative intensities of competition affecting the respective stands. The distance between curves would gauge the cumulative effect of the years of unequal competition intensities.

Crown Closure

The strongest relationship identified was the approximately linear progression of crown closure with age prior to A* (Eq. 20). This relationship could be used to determine the condition of a stand relative to its basal area culmination age. Unfortunately, trends in post-culmination-age CC are not as easily manipulated for basal area prediction. From the results reported, crown closure could be used to determine basal area culmination age in the following manner. For a given spacing, CC* would be predicted from a model such as Eq. (22). The pre-culmination Age-CC model (Eq. 20) would be used to ascertain the time differential between the current (pre-culmination) CC and the predicted CC*. This model would possess limited utility, however, because knowledge of spacing and site index could be used to gain the same information.

The only method of determining post-A* stand conditions suggested by the results involves the MO index. Essentially, any detectable multiple overlapping indicates the presence of competition effects on basal area growth. This information may be of limited use, however, because information about the age of culmination relative to the current (post-culmination) age may or may not be obtainable. Development of a post-culmination model based on MO was not pursued here, because such an approach seemed impractical in terms of both modeling precision and data collection.

The topic of data collection is an issue, not only because it relates to the quality of data used in this study, but because it may limit the applicability of any models presented herein. Measuring live crowns from ground-level gets progressively more difficult and prone to error as the trees increase in size. On the spacing trials, crown widths were measured to the nearest tenth of a foot through age 5. At ages 6-8, widths were taken to the nearest foot. At ages 9-10 and 12 widths were measured to the nearest half-meter ($\approx$ 1.6 ft). These changes in measurement precision coincide roughly with the ability of an observer on the ground to pinpoint the location of a branch overhead. Systematic error may be introduced by the fact that the bases of the live crowns of closely-spaced trees are significantly higher than those of widely-spaced trees of the same height. On the spacing trials, fortunately, the most precise (and presumably accurate) crown measurements were made on the youngest trees. This fact bodes well for a study which looks closely at crown dynamics prior to the age of basal area culmination.

Another point of importance is that measurement of individual tree crowns is not necessarily the most accurate or efficient way to determine stand crown closure (CC). Individual crown measurements were taken from ground-level on the spacing trials because the data were

intended for a variety of research applications. Given the limitations of the elliptical shape assumption, it is quite feasible to derive crown closure from individual tree measurements; however, the converse statement would not be true. A number of methods have been employed to determine crown closure from the ground or overhead. None of these, to my knowledge, have been refined specifically for determining crown overlap (CO, MO) or the total projection area (CAP) of live crowns. Possibilities do exist, however, for such refinements. The sighting tube method described by Ganey and Block (1994), for instance, could be modified to tally overhead coverage by multiple trees.

Time-correlated variations in crown closure apparent in the data (Fig. 7) spawn some concern for the potential problems they might impose on this modeling approach; furthermore, some understanding of the factors which cause these trends - be they biological or environmental - would be beneficial. The most conspicuous cause seems to be environmental. Certain climate stresses which may have affected entire sites or the entire study region could easily account for the presence of simultaneous reductions in outward crown growth. Also, there may be biophysical properties of the species that cause step-like behavior in the outward growth of crowns. One-such property that is clear from individual tree data is the tendency of projection areas to swell and shrink cyclically. Such cycles are undoubtedly linked to the phenomena of branch mortality and upward crown-recession. Impacts to the modeling approach are conspicuous for the later stages of data collected here, but early-age environmental (and perhaps biophysical) impacts ultimately end up as noise in the model.

The ice damage experienced at the upper Piedmont site is a glaring example of the magnitude of noise that environmental factors can introduce into a model. One only has to glance at the coefficients of variation for mean CC at age 12 for the four sites (.365, .077, .069, .129) to see that something is wrong with the first one in the list. The data screening performed here was minimal, but gave results that were purposeful. Had the ice-damage occurred at an earlier age or the models been more sensitive to it, useful results may have been unobtainable. As it stands, the impact of this problem has been largely unstudied in the context of the current study. The findings of Amateis and Burkhart (1996) were used to make some cursory assessment of the degree to which data culling should be carried out, but some data from damaged trees surely endured the screening process.

Crown Closure at Basal Area Culmination Age

Perhaps the most interesting result from the crown closure analysis involves the lack of significance - especially for square-spacing data only - of site index or location variables in explaining CC*. This result was unexpected, but not surprising in retrospect. Clearly, crown closure is elevated on high-quality juvenile sites. Eq. (20) tells us that a site index differential of 10 feet translates to roughly 17.1 percent higher crown closure on pre-culmination-age plots. Furthermore, increases in the site index predictor drive culmination ages downward on high-quality sites. Ostensibly, these responses offset each other at the point of their intersection: CC*.

Thus, the notion that CC* is unchanged by site index is supported both theoretically and by the results of this rudimentary statistical analysis.

The effect of spacing on CC* is another interesting result. That narrowly spaced plots support a higher degree of crown closure at A* might lead to the conclusion that they can support a greater amount of foliage before exhibiting BA competition effects. Before drawing such a conclusion, however, it would be advantageous to study the behavior of crown heights or overall crown volume at A*. Still, the direct relationship between number of trees and CC* is so prominent that it would not be surprising to find a similar relationship between number of trees and total crown volume at A*.

Effects of Rectangularity

Zhang et al. (1996) used an index of rectangularity $R=\frac{WRD}{BRD}$ to conclude that rectangularity has a negligible effect on height and diameter growth in the spacing trial. Their results indicate that it is unnecessary to account for rectangularity in basal area models, so perhaps the use of the GS variable in predicting A* was sufficient. To be sure, rectangularity effects on culmination age were not as visibly apparent as its effects on crown closure. However, the fact that the regression of A* on growing space and site index fitted to square-spacings only (Eq. 23) had a substantially improved fit over the fit to all data (Eq. 18) would seem to leave the question unanswered. In any case, the result was clear for the crown closure response. Although the impact of rectangularity was not quantified, extreme rectangularity certainly reduced crown closure and increased crown overlap for a given area of growing space.

One final point is relevant regarding the use of the growing-space variable (GS). This variable closely mimics what is commonly called "planting density", but there is one notable difference. Planting density, or number of stems planted (N_o) is generally considerably higher than the surviving numbers of stems at ages 2, 3, 4, etc., because of mortality related to transplantation and the earliest stages of stand development. Such mortality was greatly reduced on the spacing trials by conscientious efforts at replanting unsuccessfully transplanted stems. In a sense, the GS variable may more closely resemble the commonly used stems per acre (N_{age}) variable, which accounts for trees surviving at a given age. Mortality is present in the spacing trials, however, thus N_{age} is variable with time. The static GS variable can be considered some type of intermediate between N_o and N_{age}. The use of this variable does not likely vitiate the findings of the study, because it is so closely associated with both of the more commonly used predictors.

Chapter 6

CONCLUSIONS

Increasing intensity of forest management, especially shortened rotation ages, will require increased ability to model early-stand conditions. Past efforts at modeling growth and yield focused mainly on the merchantable stages of stand development. As such, they treated the culmination of basal area increment as a fairly unimportant consideration. However, a better understanding of this characteristic could be exploited to develop more exact models. An investigation into basal area culmination and its relation to various crown closure indices was the primary goal of this study.

A number of objectives were made practical by the quality of data available from spacing trials carried out by the Loblolly Pine Growth and Yield Research Cooperative. Among these were the development of basal area growth curves that could be used to determine the age of basal area culmination. Abundant crown measurements made it possible to investigate crown closure relationships to basal area prior to and at the culmination age. The factorial arrangement of four levels of spacing and blocking by location facilitated the study of spacing and site effects on these relationships.

Culmination age was found to vary inversely with both stem density and site index. A proposed functional relationship could be used to model the response across the possible range of spacings. It was noted that for certain narrow spacing conditions, basal area growth curves will no longer follow a sigmoidal path - namely, they will lose their inflection point. Formulation of the basal area models led to certain problems related to the number of surviving stems per acre (N) that are taller than breast height. Since N is variable with age, it influences the inflection point of the model. As such, it was impossible to derive compatible estimates of per-acre and average basal area culmination ages. The per acre estimates were considered conservative indicators of the age at which basal area growth is reduced by intraspecific competition.

Crown closure was elevated on high-quality sites, and exhibited an approximately linear increase with time from planting until the age of basal area culmination. Growing space effects on the slope of the increases were found to be significant, as seen from the following equation (r^2=0.791).

$$CC = -1.147 + 0.177(Age) + 0.0171(SI) - 0.000723(GS*Age)$$

where

Age - years since planting
SI - site index, ft (base age 25)
GS - average growing space at planting, ft^2

This and other equations developed could be used to predict the age at which culmination would occur, and the crown closure at that age, possibly relating these predictions to the current stand conditions.

A significant finding of the study was that crown closure at the time of basal area culmination is dependent on initial spacing, but independent of site differences. The dependence on spacing encourages questions about trends that would be found if the study was expanded to include crown height or crown volume variables. Other results involved the similarity between accuracy of three edge-bias compensation methods, and a modification to the Schnute growth model that constrains it to an initial size zero at some initial age.

RECOMMENDATIONS

The following is a list of recommended topics for further study stimulated by the research conducted herein, and introduced in earlier sections of this thesis:

- Verification of the independence of CC* and site quality
- Exploration of other crown variables' relationships to basal area growth and culmination
- More exact determination of the onset of basal area competition
- Development of post-culmination-age crown-dynamic models
- Search for a better means of correlating site characteristics to early stand characteristics
- Investigation of the relationship between mean-tree and whole stand basal area, especially with regard to what I have referred to as the "recruitment" effect

LITERATURE CITED

Amateis, R. L., and H. E. Burkhart. 1996. Impact of heavy glaze on a set of loblolly pine spacing trials. Southern Journal of Applied Forestry. In press.

Amateis, R. L., H. E. Burkhart, and S. M. Zedaker. 1987. Experimental design and early analyses for a set of loblolly pine spacing trials. In: Ek, A. R., S. R.Shifley, and T. E. Burk, eds. *IUFRO Forest Growth Modelling and Prediction Conference*. USDA Forest Service. North Central Forest Experiment Station General Technical Report NC-120. pp. 1058-1065.

Amateis, R. L., P. J. Radtke, and H. E. Burkhart. 1995. TAUYIELD: A stand-level growth and yield model for thinned and unthinned loblolly pine plantations. Loblolly Pine Growth and Yield Research Cooperative Report No. 82. 38 p.

Arney, J. D. 1972. Computer simulation of Douglas-fir tree and stand growth. Unpublished Ph. D. Thesis, Oregon State University. 79 p.

Assmann, E. 1970. The principles of forest yield study. Pergamon Press. New York. 506 p.

Avery, T. E., and H. E. Burkhart. 1994. Forest measurements. 3d ed. McGraw-Hill Inc. New York. 408 p.

Bates, D. M., and D. G. Watts. 1988. Nonlinear regression analysis and its applications. John Wiley and Sons. New York. 365 p.

Bella, I. E. 1971. A new competition model for individual trees. Forest Science. 17:364-372.

Boyer, W. D. 1970. Shoot growth patterns of young loblolly pine. Forest Science. 16: 472-482.

Bredenkamp, B. V., and T. G. Gregoire. 1988. A forestry application of Schnute's generalized growth function. Forest Science. 34:790-797.

Burton, J. D., and E. Shoulders. 1982. Crown size and stand density determine periodic growth in loblolly pine plantations. In: E. Jones, ed. *Second Biennial Southern Silvicultural Research Conference*. USDA Forest Service. South East Forest Experiment Station General Technical Report SE-24. pp. 283-287.

Chapman, D. G. 1961. Statistical problems in dynamics of exploited fisheries populations. In: J. Neyman, ed. *Proceedings of the Fourth Berkeley Symposium on Mathematical Statistics and Probability*. University of California Press. Vol. 4. pp. 153-168.

Clutter, J. L. 1963. Compatible growth and yield models for loblolly pine. Forest Science 9:354-371.

Daniels, R. F. and H. E. Burkhart. 1975. Simulation of individual tree growth and stand development in managed loblolly pine plantations. Division of Forestry and Wildlife Resources. Virginia Polytechnic Institute and State University. FWS-5-75. 69 p.

Daniels, R. F., H. E. Burkhart, and T. R. Clason. 1986. A comparison of competition measures for predicting growth of loblolly pine. Canadian Journal of Forest Research. 16:1230-1237.

Daubenmire, R. 1959. A canopy-coverage method of vegetation analysis. Northwest Science. 33:43-64.

Evans, G. C., and D. E. Coombe. 1959. Hemispherical and woodland canopy photography and the light climate. Journal of Ecology. 47:103-113.

Ek, A. R., and R. A. Monserud. 1974. FOREST: A computer model for simulating growth and reproduction of mixed species forest stands. University of Wisconsin School of Natural Resources Research Report. R2635. 13 p.

Ganey, J. L., and W. M. Block. 1994. A comparison of two techniques for measuring canopy closure. Western Journal of Applied Forestry. 9:21-23.

Griffing, C. G., and W. W. Elam. 1971. Height growth patterns of loblolly pine saplings. Forest Science 17:52-54.

Harrison, W. C., and R. F. Daniels. 1987. A new biomathematical model for growth and yield of loblolly pine plantations. In: A. R. Ek, S. R. Shifley and T. E. Burk, ed. *Forest Growth Modelling and Prediction*. USDA Forest Service. North Central Forest Experiment Station General Technical Report NC-120. pp. 293-304.

Hatch, C. R. 1971. Simulation of an even-aged red pine stand in Northern Minnesota. Ph.D. thesis, University of Minnesota, St. Paul, Minnesota. University Microfilms. 72-14,314.

Huang, S., S. J. Titus, and D. P. Wiens. 1992. Comparison of nonlinear height-diameter functions for major Alberta tree species. Canadian Journal of Forest Research. 22:1297-1304.

Hunt, R. 1982. Plant growth curves - the functional approach to plant growth analysis. Edward Arnold. London. 248 p.

Husch, B., C. I. Miller, and T. W. Beers. 1982. Forest mensuration. 3d ed. John Wiley and Sons. New York. 402 p.

James, F. C., and H. H. Schugart Jr. 1970. A quantitative method of habitat description. Audubon Field Notes. 24:727-736.

Kramer, P. J. 1943. Amount and duration of growth of various species of tree seedlings. Plant Physiology. 18:239-251.

Lanner, R. M. 1976. Patterns of shoot development in *Pinus* and their relationship to growth potential. In: G. R. Cannell and F. T. Last, ed. *Tree physiology and yield improvement*. Academic Press. New York. pp. 223-243.

Lemmon, P. E. 1956. A spherical densiometer for estimating forest overstory density. Forest Science. 2:314-320.

Lin, C. and P. M. Morse. 1975. A compact design for spacing experiments. Biometrics. 31:661-671.

Mitchell, K. J. 1975. Stand description and growth simulation from low-level stereo photos of tree crowns. Journal of Forestry. 73:12-16.

Monserud, R. A., and A. R. Ek. 1974. Plot edge bias in forest stand growth simulation models. Canadian Journal of Forest Research. 4:419-423.

Pienaar, L. V., and K. J. Turnbull. 1973. The Chapman-Richards generalization of Von Bertalanffy's growth model for basal area growth and yield in even-aged stands. Forest Science. 19:2-22.

Pütter, A. 1920. Studien über physiologische Ähnlichkeit. VI. Wachstums-ähnlicjkeiten. Pflügers Arch. ges. Physiol. 180:298-340.

Reynolds, M. R. 1984. Estimating the error in model predictions. Forest Science. 30:454-468.

Richards, F. J. 1959. A flexible growth function for empirical use. Journal of Experimental Botany. 10(29):290-300.

Schnute, J. 1981. A versatile growth model with statistically stable parameters. Can. J. Fish. Aquat. Sci. 38:1128-1140.

Seber, G. A. F., and C.J. Wild. 1989. Nonlinear regression. John Wiley and Sons. New York. 768 p.

Sit, V. and M. Poulin-Costello. 1994. Catalog of Curves for Curve Fitting. Biometrics Information Handbook Series. No. 4. Edited by Wendy Bergerud and Vera Sit. British Columbia Ministry of Forests. Crown Publications Inc. Victoria, B.C. 110 p.

Spurr, Stephen H., 1960. Photogrammetry and photo-interpretation. 2d ed. The Ronald Press Co. New York. 472 p.

Strub, M. R., R. B. Vasey, and H. E. Burkhart. 1975. Comparison of diameter growth and crown competition factor in loblolly pine plantations. Forest Science. 21:427-431.

Von Bertalanffy, L. 1938. A quantitative theory of organic growth (Inquiries on growth laws II). Human Biology 10:181-213.

Von Bertalanffy, L. 1957. Quantitative laws in metabolism and growth. The Quarterly Review of Biology. 32:217-231

Zeide, B. 1989. Accuracy of equations describing diameter growth. Canadian Journal of Forest Resources. 19:1283-1286.

Zeide, B. 1993. Analysis of growth equations. Forest Science. 39:594-616.

Zhang, S., H. E. Burkhart, and R. L. Amateis. 1996. Modeling individual tree growth for juvenile loblolly pine plantations. Loblolly Pine Growth and Yield Research Cooperative Report No. 89. 38 p.

Appendix A

Mathematical Relationship Between A^*_{QMD} and A^*

The relationship between QMD and BA was given as

$$QMD = \left[\frac{BA}{N\,(0.005454154)}\right]^{\frac{1}{2}} \tag{A1}$$

Substituting the Richards BA growth model into Eq. (A1) gives

$$QMD = \left(\frac{a}{N\,(0.005454154)}\right)^{\frac{1}{2}}\left(1 - e^{b(Age - A_o)}\right)^{\frac{c}{2}} \tag{A2}$$

Let N be fixed with respect to age and $c > 2$. Then the inflection age, A^*_{QMD}, of Eq. (A2) will always be smaller than the inflection age of the corresponding BA curve.

$$A^*_{QMD} = A_o + \frac{1}{b}\ln\left(\frac{2}{c}\right) < A^* = A_o + \frac{1}{b}\ln\left(\frac{1}{c}\right) \tag{A3}$$

This is the basis for the result that fitting QMD data to the Richards model gave A^*_{QMD} estimates considerably smaller than the per acre basal area culmination age estimates.

Working with mean-tree basal area rather than mean-tree diameter gives

$$\overline{BA} = \frac{a}{N}\left(1 - e^{b(Age - A_o)}\right)^{c} \tag{A4}$$

which shares a common inflection point (constant N) with per acre basal area ($A^* = A^*_{\overline{BA}}$). Note that N is not constant with respect to Age, complicating the relationship between BA and $\overline{BA}$ culmination ages.

VITA

Philip J. Radtke was born on October 27, 1965 in Marshfield, Wisconsin to parents Robert J. and Phyllis M. (Ruder) Radtke. He earned an Associate degree in Restaurant and Hotel Cookery at the Madison Area Technical College in Madison, Wisconsin in 1990. In 1994 he completed a Bachelor of Science degree in Natural Resources and Environmental Studies at the University of Minnesota, Twin Cites. Upon graduation, he entered the graduate school at Virginia Polytechnic Institute and State University in Blacksburg, Virginia, where he earned a Master of Science degree in Forestry in 1996.